



저작자표시-비영리-변경금지 2.0 대한민국

이용자는 아래의 조건을 따르는 경우에 한하여 자유롭게

- 이 저작물을 복제, 배포, 전송, 전시, 공연 및 방송할 수 있습니다.

다음과 같은 조건을 따라야 합니다:



저작자표시. 귀하는 원저작자를 표시하여야 합니다.



비영리. 귀하는 이 저작물을 영리 목적으로 이용할 수 없습니다.



변경금지. 귀하는 이 저작물을 개작, 변형 또는 가공할 수 없습니다.

- 귀하는, 이 저작물의 재이용이나 배포의 경우, 이 저작물에 적용된 이용허락조건을 명확하게 나타내어야 합니다.
- 저작권자로부터 별도의 허가를 받으면 이러한 조건들은 적용되지 않습니다.

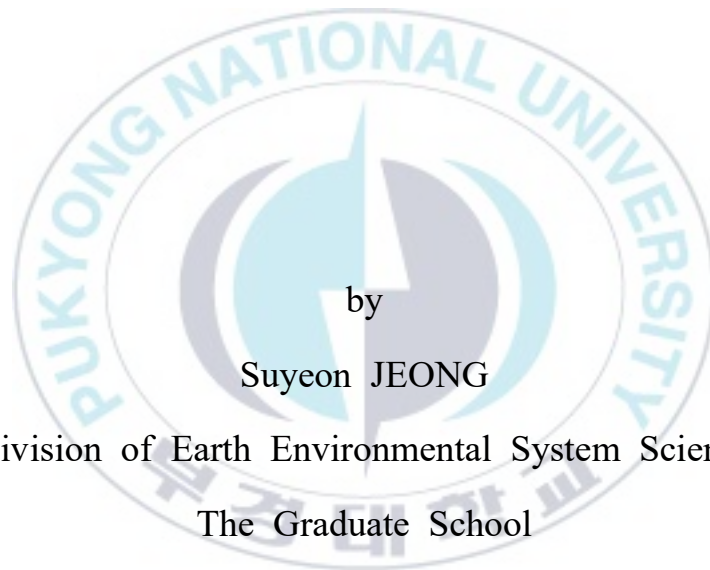
저작권법에 따른 이용자의 권리는 위의 내용에 의하여 영향을 받지 않습니다.

이것은 [이용허락규약\(Legal Code\)](#)을 이해하기 쉽게 요약한 것입니다.

[Disclaimer](#)

Thesis for the Degree of Master of Science

# Present and Future of Volume Transport through the Korea Strait



by

Suyeon JEONG

Division of Earth Environmental System Science

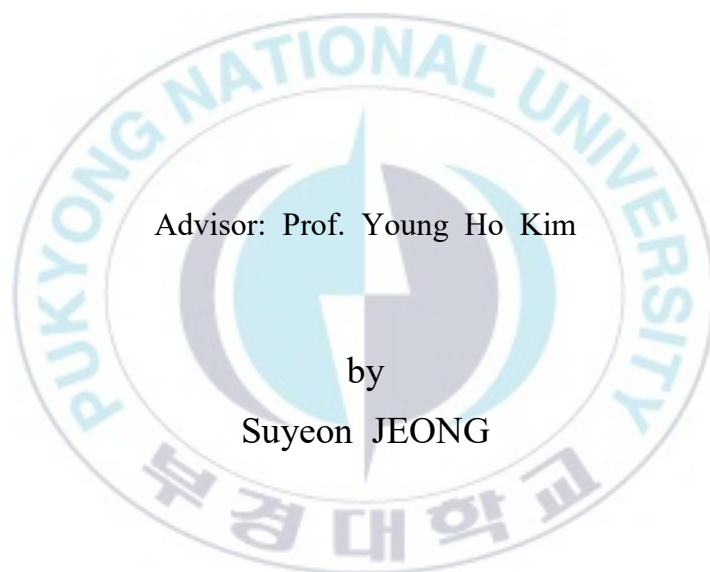
The Graduate School

Pukyong National University

February 2023

Present and Future of Volume Transport through  
the Korea Strait

대한해협 수송량의 현재와 미래



Advisor: Prof. Young Ho Kim

by

Suyeon JEONG

A thesis submitted in partial fulfillment of the requirements  
for the degree of

Master of Science

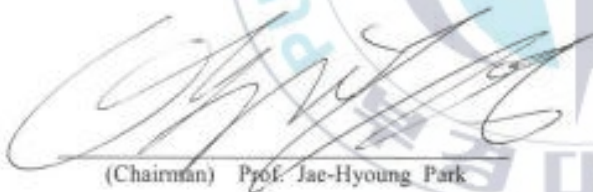
in Division of Earth Environmental System Science, The Graduate School,  
Pukyong National University

February 2023

Present and Future of Volume Transport through the Korea Strait

A thesis  
by  
Suyeon JEONG

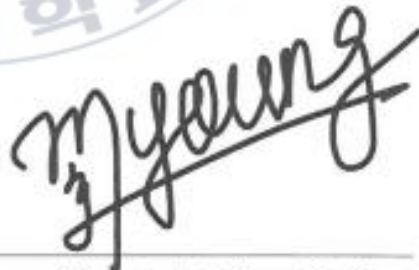
Approved by :



(Chairman) Prof. Jae-Hyoung Park



(Member) Ph.D. Young-Gyu Kim



(Member) Prof. Young Ho Kim

February 17, 2023

## Contents

Abstract .....	iii
List of Tables .....	vi
List of Figures .....	vii
I. Introduction .....	1
II. Data and Method .....	7
1. Observation Data of Korea Strait .....	7
2. Observation Data of Tokara Strait .....	17
3. Reanalysis Data .....	19
4. CMIP6 Data .....	26
5. Phase Spectrum .....	33
6. Coherence Spectrum (Coherency) .....	34
III. Results .....	35
1. The volume transport of Korea Strait .....	35
2. Relationship between Korea Strait and Tokara Strait .....	47
3. CMIP6 .....	61

IV. Conclusion and Discussion .....	69
Abstract(Korean) .....	72
Reference .....	75
Acknowledgements .....	90



Present and Future of Volume Transport through the Korea Strait

Suyeon JEONG

Division of Earth Environmental System Science  
The Graduate School, Pukyong National University

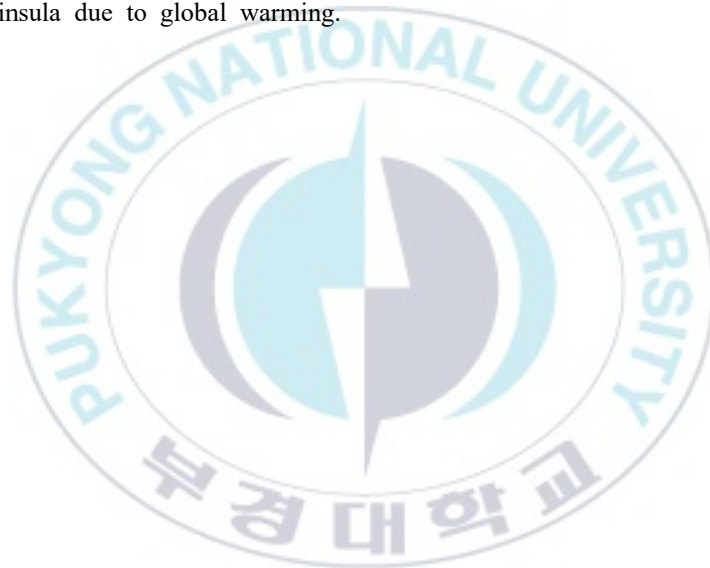
**Abstract**

Tsushima Warm Current(TWC) through the Korea Strait transports heat, salt, and other physical properties to the East Sea. Thus, the volume transport in Korea Strait must be studied. As the Tsushima Warm Current is a branch of the Kuroshio Current, it is important to find out the relationship with the Kuroshio Current in order to study the volume transport in the Korea Strait. In this study, ADCP observations and high-resolution reanalysis data such as GLORYS, HYCOM, and OPEM were used for analysis. To obtain current data which tidal components were removed from the ADCP mounted on the Camellia ferry, which travels between Hakata, Japan and Busan, Korea, the route of the observation was newly set using the least squares method, and 14 tidal components were calculated through the

harmonic analysis. In addition, in order to estimate surface and bottom ocean currents, which are difficult to observe, we tried to find an extrapolation method suitable for the ADCP data of Camellia ferry using ADCP data observed at NRL. The gradient extrapolation was judged to be the best fit, and gradient extrapolation was performed in the bottom layer, and the surface layer was extrapolated using the observed values of the first layer. As a result, from the Camellia ADCP data, the volume transport of the Korea Strait is about 2.69 Sv in average, and the volume transport through the western channel and eastern channel are estimated to be about 1.34 Sv and about 1.45 Sv, respectively. As a result of the analysis, it was found that the volume transport in the Korea Strait has increased over time. In addition, to investigate the relationship between the Korea Strait and the Kuroshio Current, correlation and spectrum analysis between the Korea Strait and the Tokara Strait were performed. The correlation coefficient between volume transport in Korea Strait and Tokara Strait was found to be  $-0.76$ . Coherence spectrum analysis using reanalysis data showed that the volume transport through the Tokara Strait leads that through the Korea Strait for about 2 months in a 5-month frequency.

In addition, the results of 10 CMIP6 models were analyzed to find out the relationship between the Korea Strait and the Kuroshio Current in the future climate. In scenarios where radiative forcing becomes stronger, the Kuroshio Current moved northward, the Korea Strait transport increased and the Tokara Strait transport decreased from 2090 to 2100. The boundary of circulation is marked by zero-windstress curl and the mean latitude of the Hadley Circulation in mid-latitude is also moving poleward as global warming progresses, as confirmed by ERA5 data over the past 30 years. The poleward of the Hadley circulation affects the poleward

of the Kuroshio Current, which can be interpreted as the cause of the poleward movement of the Kuroshio extension. As a result, the volume transport of the Tsushima Warm Current entering the Korea Strait is expected to increase, while the volume transport of Kuroshio Current through the Tokara Strait is expected to decrease. The increasing volume transport of the Tsushima Warm Current has increased the sea surface temperature around the Korean Peninsula, which may change the oceanic circulation and hydrographic condition in the marginal seas around the Korean Peninsula due to global warming.



## List of Tables

<b>Table. 1</b> Previous research about volume transport in Korea Strait with method. ....	5
<b>Table. 2</b> Data used in this study. ....	23
<b>Table. 3</b> Modeling centers and their model(s) used for this study with ocean grid and DOIs. ....	28
<b>Table. 4</b> The total volume transport and those in the western channel and eastern channel in Korea Strait from 2004 to 2019. ....	45
<b>Table. 5</b> Ensemble mean of volume transport of each scenario in Korea Strait and Tokara Strait from 2090 to 2100. ....	65

## List of Figures

- Figure. 1** Current near Korea Peninsula and Korea Strait and Tokara Strait are the region of this study. .... 6
- Figure. 2** Every route the Ferry Camellia and the black line and dot are the new route to be estimated using the least squares method. .... 9
- Figure. 3** The relationship between the transducer beam angle and the thickness of the contaminated layer at the surface (Teledyne RD Instruments, 2011). ... 14
- Figure. 4** Example of how data are extrapolated by the three methods. The black denotes the NRL observation data, and the aqua denotes the last two observation depths in the ship-mounted data. The blue, red, and green denote the first, second, and third extrapolation methods, respectively. .... 14
- Figure. 5** Methods of extrapolation. Method 1 uses same value of the last bin. Method 2 uses gradient extrapolation and Method 3 uses linear extrapolation assuming that the bottom velocity is 0. .... 15
- Figure. 6** Percent of extrapolation using bottom-mounted ADCP. .... 15

<b>Figure. 7</b> The route of the Ferry Camellia operated and the position of the bottom-mounted ADCP in the North section which was used to find the method of extrapolation. ....	18
<b>Figure. 8</b> Flow chart how to deal with the ship-mounted ADCP data. ....	25
<b>Figure. 9</b> 18m monthly mean velocity from January to April. ....	38
<b>Figure. 10</b> 18m monthly mean velocity from May to August. ....	39
<b>Figure. 11</b> 18m monthly mean velocity from September to December. ....	40
<b>Figure. 12</b> The yearly mean velocity of observation data from 2004 to 2011. Whole year mean data are not available for 2004. ....	41
<b>Figure. 13</b> The yearly mean velocity of observation data from 2012 to 2019. ....	42
<b>Figure. 14</b> Climatology of observation data in Korea Strait from 2005 to 2019. ....	43
<b>Figure. 15</b> Volume transport in Korea Strait (WC denotes western channel and EC denotes eastern channel of Korea Strait) and volume transport observed by Shin et al. (2022) ....	44

**Figure. 16** The volume transport of Korea Strait with trend line in reanalysis data and observation data. The blue color denotes GLORYS, lime color denotes HYCOM, yellow color denotes OPEM and the red color express the observation data which is dealt with this study. .... 46

**Figure. 17** Yearly volume transport of Korea Strait from 2005 to 2019 and that of Tokara Strait from 1992 to 2015 ..... 50

**Figure. 18** Yearly volume transport of observation data from 1993 to 2015 and reanalysis data from 1994 to 2017 in Tokara Strait. .... 51

**Figure. 19** The volume transport of reanalysis data in Korea Strait and Tokara Strait. .... 52

**Figure. 20** The yearly anomaly volume transport in observation data(red) and reanalysis data. The blue color denotes GLORYS, lime color denotes HYCOM and yellow color denotes OPEM. KS and KT are abbreviation of Korea Strait transport and Kuroshio Current Transport respectively. .... 53

**Figure. 21** The volume transport in Korea Strait(above) and Tokara Strait(bottom). The blue color denotes GLORYS, lime color denotes HYCOM, yellow color denotes OPEM and red color denotes the observation data which deal with this study. .... 54

**Figure. 22** The volume transport of reanalysis time series data. The blue color denotes the GLORYS, green color denotes the HYCOM and the yellow color denotes the OPEM, and the solid and dotted lines denote the volume transports of Korea Strait and Tokara Strait, respectively. .... 55

**Figure. 23** Monthly lag correlation in GLORYS(blue), HYCOM(lime) and OPEM(yellow). .... 58

**Figure. 24** Cross spectral density using monthly reanalysis data. .... 59

**Figure. 25** Coherence and phase (+) between monthly time series in GLORYS (blue), HYCOM (lime), and OPEM (yellow). The gray vertical lines show the highest coherence vector in each model, and red horizontal line denotes the 95% confidence level in coherence spectrum. .... 60

**Figure. 26** Volume transport of Korea Strait from 2090 to 2100. .... 64

**Figure. 27** Volume transport of Tokara Strait from 2090 to 2100. .... 65

**Figure. 28** Sea Surface Temperature (a) and surface current (b) change (2091-2100) according to ScenarioMIPs from each historical simulations (2005-2014) from ensemble mean of 9 models (KIOST-ESM, MRI-ESM2.0, INM-CM4.8, INM-CM5.0, IPSL-CM6A-LR, GISS-E2.1-G, EC-Earth3,

CNRM-ESM2.1, ACCESS-CM2). Left, middle, right panels denote SSP1-2.6, SSP2-4.5, SSP5-8.5 respectively (정 등,2021). ..... 66

**Figure. 29** Time series of zero windstress curl latitude in mid-latitude of the North Pacific (10-year running average) from ERA5 observation and ScenarioMIPs of 9 models. (a) ERA5 reanalysis (observation), (b) ScenarioMIP SSP1-2.6, (c) ScenarioMIP SSP2-4.5, (d) ScenarioMIP SSP5-8.5. (정 등,2021). ..... 67

**Figure. 30** Volume transport of the Tsushima Warm Current through the Korea Strait for historical simulations (2005-2014) and ScenarioMIP simulations (2091-2100) (정 등,2021). ..... 68



## I . Introduction

The Korea Strait connects the East Sea and the East China Sea (ECS) and has a width, length, and mean water depth of about 180 km, 330 km, and 100 m, respectively (Takikawa et al, 2003). The Tsushima Warm Current (TWC) flows through the Korea strait into the East Sea, greatly influencing its circulation through the transport of heat, salt, and momentum. Therefore, it is essential to understand the vertical current structure of Korea Strait and the volume transport through the strait. Additionally, to model the circulation in the East Sea as accurately as possible, accurate inflow data such as current, temperature and salinity are required for the Korea Straits (Takikawa et al, 2003).

The TWC splits into two distinct branches when it enters the East Sea. One branch passes through the western channel, located along the Korean coast, whereas the other branch passes through the eastern channel, located along the Japanese coast. The current direction in the strait is generally toward the East Sea; however, there are countercurrents with a dipole of eddies in the downstream near the Tsushima Islands (Lee et al., 2015; Takikawa et al., 2005).

Long-term measurements of currents in the Korea Strait have been difficult to obtain and have been almost nonexistent due to the intense level of fishing and trawling (Kawatate et al., 1988). Short-term current observations have shown strong currents with large tidal components (Mizuno et al, 1989; Egawa et al, 1993; Isobe et al, 1994; Katoh et al, 1996). In a joint effort by Japan,

Korea, and the U.S. to study the East Asian Marginal Seas, the United States Naval Research Laboratory (NRL), as part of its Dynamical Linkages of Asian Marginal Seas (LINKS) program, deployed 12 ADCPs in TRBMs for 11 months in the Korea Strait during 1999–2000 (Perkins et al, 2000a; Teague et al, 2002).

Considerable research has been conducted to estimate the volume transport in Korea Strait. Yi et al. (1966) used sea level variations measured with tide gauges at Busan, Jeju, and Izuhara to deduce a mean current of 48.5 cm/s with an annual variability of 38.5 cm/s (Jacobs et al,2001). Isobe et al. (1994) combined sea level observations on opposite sides of the strait to determine barotropic transport and used hydrographic observations to account for baroclinic compensation effects (Jacobs et al., 2001). The seasonal transport variability of 0.7 Sv is estimated through this method (Jacobs et al,2001). Several studies have attempted to estimate the volume transport in Korea Strait, as shown in Table 1. Ship-mounted ADCP and tide gauge are the most used observation data to calculate the volume transport in Korea Strait and there are over 2 Sv in general (Table 1).

There are more long-term ship-mounted ADCP data obtained by Kyushu University in recent collaboration with Pukyong National University. It operated Ferry New Camellia from July 2004 to December 2019 for six or seven times a week. The total volume transport of Korea Strait is 2.65 Sv and 1.21 Sv, 1.45 Sv in eastern channel and western channel, respectively (Fukudome et al, 2010).

The Tokara Strait to the south of Kyushu Island is a choke point in the

Kuroshio stream, and significant heat, nutrients, and organic matter are carried by the Kuroshio from the ECS into the North Pacific through the Tokara Strait (Liu et al, 2021; Feng et al., 2000; Nakamura et al., 2003; Nitani, 1972) (Figure 1).

The Kuroshio current axis toward poleward tends to make the current flows along the isobaths near the Tokara Strait and then more current flows enters the Korea Strait in Andres et al. (2009). Shin et al. (2021) revealed a negative correlation between volume transport of Korea Strait and volume transport of Tokara Strait.

The northward shift in Kuroshio and Kuroshio Extension axes is a driver of increasing Kuroshio adjacent to the coast for the long-term trend in TWC transport (Kida et al, 2020). Liu et al. (2021) showed that the yearly mean Kuroshio volume transport increased when the Kuroshio axis position was northward. When the more Kuroshio axis position is northward, the more ocean current flows across the Korea Strait, as described by Andres et al. (2009). As the Kuroshio axis shifts poleward, more of the Tsushima current enters the Korea Strait. Thus, the transport volume of the Tokara Strait was analyzed by considering the transport volume of the Kuroshio Current.

TWC into the East Sea through the Korea Strait also might have increased as the atmospheric radioactive forcing increased in Coupled Climate Model Inter-comparison Project Phase 6 (CMIP6) (정 등, 2020). The poleward shift of Hadley Circulation should account for the poleward shift of Kuroshio current. Thus, we attempted to analyze the volume transports in Korea Strait and Tokara Strait in future climate with CMIP6.

The purpose of this study is to derive the relationship between Korea Strait and Kuroshio current through the Tokara Strait using long-term observation data and reanalysis data and to understand how volume transport change in Korea Strait for a decade. Then, we show how the volume transport of varies in Korea Strait and Tokara Strait in CMIP6 scenarios.



<b>Study</b>	<b>Transport (Sv)</b>	<b>Method</b>
Miita and Ogawa et al(1984)	4.2	Current meter
Isobe et al (1994)	2.3	Towing ADCP
Takikawa et al (1999)	2.6	Vessel-mounted ADCP
Teague et al(2002)	2.7	Bottom-mounted ADCP
Sang Jin Lyu and Kuh Kim et al.(2002)	2.5	Dynamic calculation Submarine cable voltage
Kuh Kim et al (2003)	2.5	Submarine cable voltage
Takikawa and Yoon (2004)	2.6	Vessel-mounted ADCP
Ostrovskii et al (2008)	2.77 $\pm$ 0.77	Vessel-mounted ADCP
Fukudome et al (2010)	2.65 $\pm$ 0.5	Vessel-mounted ADCP
Kang et al (2014)	2.66	Vessel-mounted ADCP
Utsumi Yuya (2018)	2.25 $\pm$ 0.2	Vessel-mounted ADCP
Shin et al (2022)	2.61-2.64	Vessel-mounted ADCP Tidal gauge Satellite altimeter

Table 1. Previous research about volume transport in Korea Strait with method.

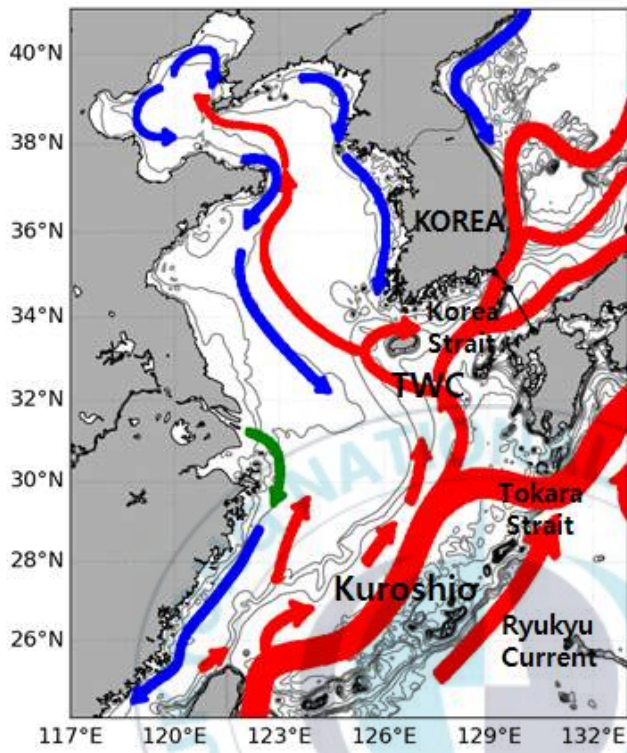


Figure 1. Current near Korea Peninsula and Korea Strait and Tokara Strait are the region of this study

## II. Data and Method

### 1. Observation Data of Korea Strait

#### Ship-mounted ADCP

Regular measurements of the currents with Acoustic Doppler Current Profiler(ADCP) mounted on the bottom of the ferry New Camellia, which cruised from Busan, Korea to Hakata, Japan were carried out 6 or 7 times a week with the ship speed of 17kt and from July 2004 to December 2019(Takikawa et al, 2005; Fukudome et al, 2010) (Table 2). The data sampling intervals were 30 s, and sampling was performed at 8 m interval from 18 m to 258 m (Takikawa et al, 2005). Data were obtained by Prof Naoki Hirose from Kyushu University, but the Ferry data did not include data from April 2011; March, April, and May 2012; April 2015; July 2017; and April and May 2018.

The ferry cannot operate the exact same route every day, and the route has to be adjusted to avoid heavy weather and bad sea conditions. Thus, it is necessary to set a new route for the ferry to operate most frequently. The least square method proposed by 内海(2018) for positioning the standard new ferry line was used in this study.

The slope of from A(Busan) and B(veering station) is  $a_1$ , the slope of from B(veering station) to C(Hakata) is  $a_2$ , the latitude of B is  $b$ , the latitude and the longitude of observation station are  $x_i, y_i$  and total number of observation

is  $N$  and  $N_1$  is the number of observation point west of veering station. The left term in the right equation is regarding the least square method in the western channel and the right term in the right equation is regarding the least square method in the eastern channel in Eqn. (1). The actual ferry routes through Korea Strait between Busan and Hakata were adjusted for avoiding heavy weather and sea conditions. The route of left side of Tsushima Island was ignored when implementing the least square method.

$$J = \sum_{j=1}^{N_1} (y_i - b - a_1 x_j)^2 + \sum_{j=N_1+1}^N (y_i - b - a_2 x_j)^2 \quad (1)$$

Because we can make cost  $J$  minimum with a differential, we can find  $a_1, a_2, b$  which make the new station. Following this result, a new station and route were set (Figure 2). The new Busan station is  $35.06^\circ N, 129.15^\circ E$ , the new veering station is  $34.70^\circ N, 129.60^\circ E$ , and new Hakata station is  $33.71^\circ N, 130.26^\circ E$  respectively. Because the total length of the new route is about 181 km, 181 horizontal segments with 1 km intervals were set. The location of the first station which is nearest Busan, called A, is A( $35.1^\circ N, 129.2^\circ E$ ) and that of the inflection peak which is the nearest station to Tsushima Island is B( $34.7^\circ N, 129.6^\circ E$ ), and that of the last station which is nearest Hakata is C( $33.7^\circ N, 130.2^\circ E$ ) (Figure 7).

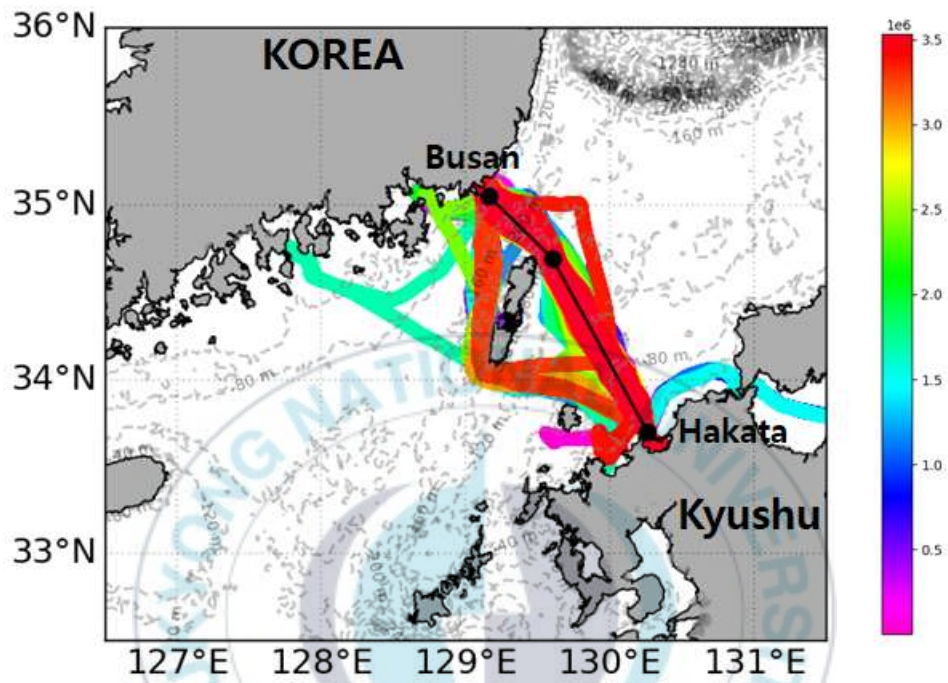


Figure 2. Every route the Ferry Camellia and the black line and dot are the new route to be estimated using the least squares method.

While the Ferry operated between Busan Port and Hakata Port, the only observation data that was used was the closet one among the 181 segments (Figure 8). Figure 8 explains the schematic flow of how the observation data was put in the closet segments. When one segment is empty, if the other data exists in the segments in the vicinity except for the closet data, that other data was put in the empty segments. As a consequence, we count one voyage which has 181 data with 30 bins of depth from Busan to Hakata and vise versa.

The Korea Strait is slanted from the North so that velocity is needed for the ferry to be rotated by the tilting angle from the North. Thus, the ship-mounted ADCP is rotated by axis transformation. Matrix rotation can express that vector  $r = (x, y)$  and vector  $R$  which is rotated by theta( $\theta$ ),  $R = (X, Y)$ . Axis rotation can express vector  $r = (x, y)$  but axis is rotated. Axis rotation is used in this study because it is better to deal with u,v velocity. Consequently, the rotation angle(theta) is  $-44.23^\circ$  in the western channel and  $-61.16^\circ$  in the eastern channel in the ship-mounted ADCP. Thus, a new velocity was set up in this study. Prior to rotate the current, the current data was filtered by the interquartile range(IQR) to look for the outliers. There are two main methods to remove outlier, one is using IQR and the other is using standard deviation. The reason why IQR is used in this study that using the standard deviation cannot eliminate the current data well.

matrix rotation

$$\begin{pmatrix} u' \\ v' \end{pmatrix} = \begin{pmatrix} \cos\theta & -\sin\theta \\ \sin\theta & \cos\theta \end{pmatrix} \begin{pmatrix} u \\ v \end{pmatrix}$$

axis transformation

$$\begin{pmatrix} u' \\ v' \end{pmatrix} = \begin{pmatrix} \cos\theta & \sin\theta \\ -\sin\theta & \cos\theta \end{pmatrix} \begin{pmatrix} u \\ v \end{pmatrix}$$

Because tidal currents are very strong and are comparable to the mean currents due to the shallow depth and narrow width of the Tsushima Strait, tidal currents must be removed from the ADCP data to study the processes associated with mean current such as mean volume transport (Fukudome et al, 2010). The major tidal constituents(Q1, O1, P1, K1, N2, M2, S2, K2, MSf, and Mf) and four additional tidal constituents ( $\mu_2$ , NO1, 1, and J1) were decomposed. In addition, to fit the tidal modes to the data, we used the ordinary least squares(OLS) method.

When experimental data are given and if researchers have to find the intervals, the method of extrapolation is used. ADCP collects acoustic pings to obtain ocean velocities. The echo from a hard surface such as the sea surface or bottom is much stronger than that from the water; thus, scattering occurs near the surface or bottom. Data obtained within 6% of the bottom depth are not reliable because the data could be contaminated by the scattering effect. Therefore, it is necessary to extrapolate for surface and bottom layer. We

considered the three types of extrapolation to identify the best method. More detailed explanations are provided below, and method 2 is explained by 内海 et al.(2018)

1. method 1 : missing velocity is same as the bottom bin velocity
2. method 2 : gradient interpolation using the degree of the last two depth velocity from bottom bin to bottom
3. method 3 : linear interpolation assuming the bottom depth velocity is zero

We used bottom-mounted ADCP data by the Naval Research Laboratory from May 1999 to March 2000 to identify the most appropriate extrapolation method to fit the data of Korea Strait. The bottom-mounted ADCP can observe more deeper depths and more shallow depths than ship-mounted ADCPs. Thus, it can be used to find the most appropriate method in the Korea Strait. Unfortunately, the ship-mounted ADCP data are not used in this section. Because the observation dates are different, it cannot be used directly to identify the extrapolation method. There is an example of how to find the closed method to the bottom-mounted ADCP (Figure 4). The black dotted line denotes the bottom-mounted ADCP, and the aqua dot denotes the last two points the ship-mounted ADCP can observe. We tried to know which extrapolation value is the closest to the deepest observation value in bottom-mounted ADCP as the closest method. We found out what percentage each method occupied in the total data (Figure 6). Thus, method 2 is the closest extrapolation method by ~50.5%. Method 3 occupied 29.5%, and

method 1 occupied 20.0%. Thus, method 2 was used to extrapolate the ship-mounted ADCP data. Surface velocity is obtained by extrapolating values in 18m.



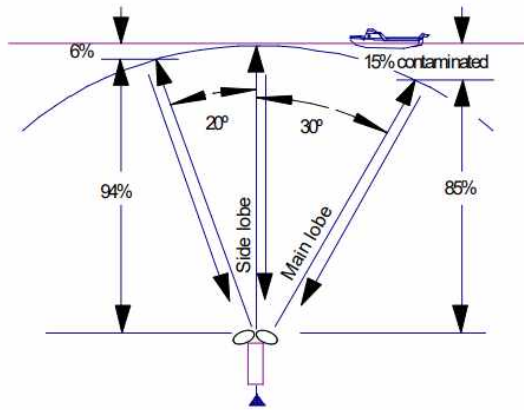


Figure 3. The relationship between the transducer beam angle and the thickness of the contaminated layer at the surface (Teledyne RD Instruments, 2011).

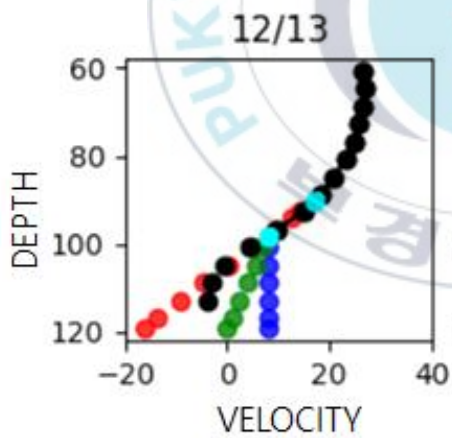


Figure 4. Example of how data are extrapolated by the three methods. The black denotes the NRL observation data, and the aqua denotes the last two observation depths in the ship-mounted data. The blue, red, and green denote the first, second, and third extrapolation methods, respectively.

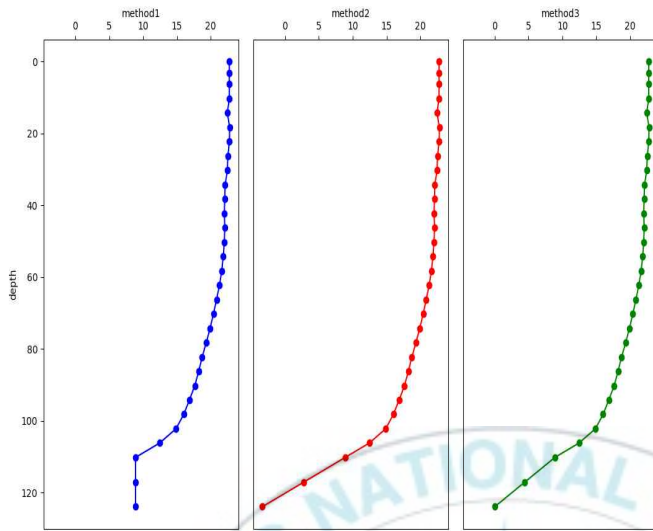


Figure 5. Methods of extrapolation. Method 1 uses same value of the last bin. Method 2 uses gradient extrapolation and Method 3 uses linear extrapolation assuming that the bottom velocity is 0.

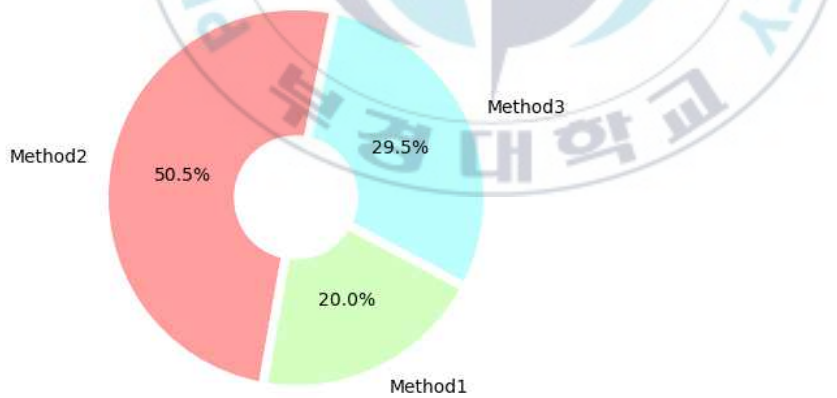


Figure 6. Percent of extrapolation using bottom-mounted ADCP.

### **Bottom-mounted ADCP**

The U.S. Naval Oceanographic Office and the Korea Ocean Research and Development Institute (KORDI) performed observations with a bottom mounted ADCP in Korea Strait from May 1999 to March 2000 (Table 2). They deployed 14 mooring packages. There are two sections to observe, one section is located northeast of Tsushima Island (mooring position denoted by N1-N6) and the other is located southwest of Tsushima Island (denoted by S1-S6)(Teague et al, 2001). All moorings were recovered and redeployed in October 1999, except those at N1 station which were not deployed in May 1999. The vertical resolution was set to 4 m, except at S1, S2, and N2 where the resolution was set to 2 m and the velocity was recorded at 30 min intervals except at 15 min intervals like that at S5, N2, and N3 (Teague et al, 2002). For the analysis of the low-frequency current, tidal currents and currents near the semidiurnal and diurnal frequencies were removed from the ADCP records using a low-pass Butterworth filter with a 40-h cutoff frequency to remove tidal currents (Teague et al, 2002). The northern line covers the outflowing current, and the southern line covers inflowing flows (Jacob et al, 2001). In this study, the northern sections close to the route of the ship-mounted ADCP were used to find the extrapolation method for the ship-mounted ADCP (Figure 2).

### **Volume transport of Korea Strait from tide gauge**

The sea level obtained by the tide gauge of Korea Hydrographic and Oceanographic Administration (KHOA) from 1975 to 2018 was used to

calculate the volume transport. The sea level data were filtered by a low-pass filter and averaged for 10 days (Shin et al, 2022). The volume transport was calculated by multiplying the geostrophic velocity. The barotropic volume transport has the same velocity when the depths are increased.

## 2. Observation data of Tokara Strait

The ferry Naminoue, measuring 145.6 m long and 22.0 m wide, was run between Kagoshima and Naze, Japan, every 4 days to investigate Kuroshio across the Tokara Strait current using a 38.4 kHz ADCP from January 2003 to March 2011 by Kagoshima University. Utilizing this dataset, Zhu et al. (2017) successfully removed the influence of tidal currents and provided more accurate absolute Kuroshio transport across the Tokara Strait than previous estimates (Liu et al, 2019). However, because we have the yearly volume transport value from 1993 to 2015, we did not process these data (Table 2).

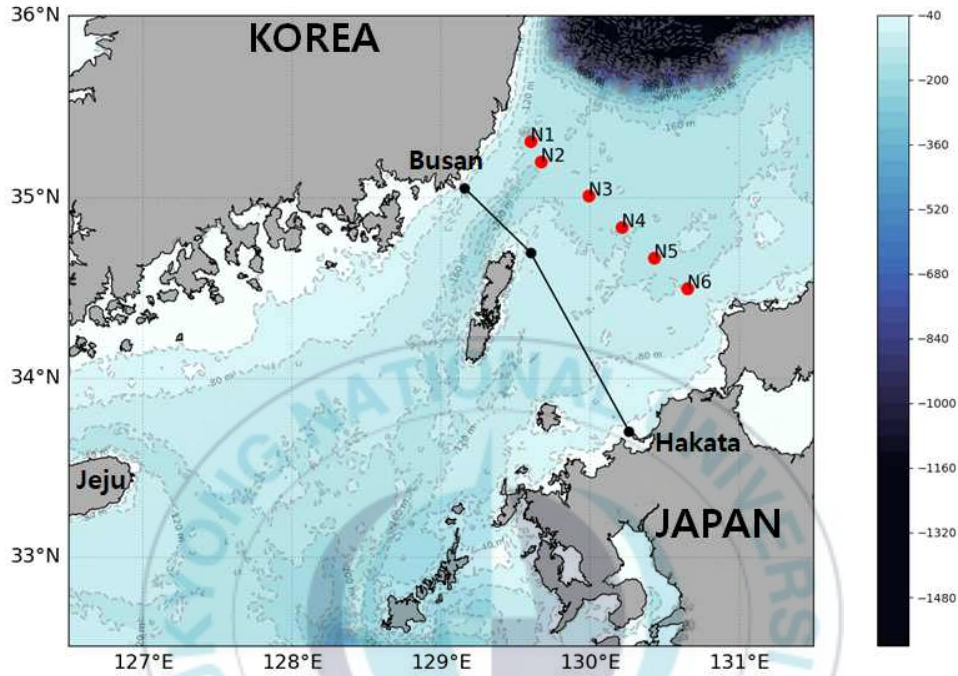


Figure 7. The route of the Ferry Camellia operated and the position of the bottom-mounted ADCP in the North section which was used to find the method of extrapolation.

### 3. Reanalysis Data

There is a growing demand for regional ocean models which are designed with the appropriate resolution and physics to represent local processes (Souza et al, 2020). Reanalysis data have a longer period than observation data and have a spatially higher resolution. Thus, it is useful to use reanalysis data for analyses during the long term and for specific regions. When multiple reanalysis data sets produce similar results, it provides confidence in the validity of the results, even in the absence of direct observations. The present work used the following three products : Copernicus Marine Environment Monitoring Service (GLORYS), HYbrid Coordinate Ocean Model (HYCOM) and Ocean Predictability Experiment for Marine Environment (OPEM).

#### **GLORYS**

The Copernicus Marine Environment Monitoring Service (CMEMS) global ocean eddy-resolving reanalysis is produced by the GLORYS12V1 product (Table 2). It has standard regular grid at  $1/12^\circ$  (approximately 8 km) and on 50 standard levels. The reanalysis is performed using the “Nucleus for European Modelling of the Ocean” (NEMO) ocean model driven by the ECMWF ERA-Interim reanalysis. It assimilates along track altimeter observations (sea level anomaly), satellite sea surface temperature (SST), sea ice concentration and in situ temperature and salinity vertical profiles from the ‘Coriolis Ocean database ReAnalysis’ (CORA) dataset (Szekely et al. 2019) using a reduced-order Kalman Filter scheme (Souza et al, 2020). Unlike the previous

hindcast simulation driven only by atmospheric conditions, an ocean reanalysis assimilates observation of oceanic variables, either derived from satellite measurements (Sea Level Anomalies, Sea Ice Concentration and Sea Surface Temperature) or in situ sampling (temperature and salinity profiles), to provide a more realistic prediction. In addition, the model has an eddy-permitting resolution, allowing a representation of mesoscale activity (Lehodey et al, 2018). The reanalysis data were used from 1994 to 2017.

### **HYCOM**

The NOAA Reanalysis-2 is based on the HYbrid Coordinate Ocean Model (HYCOM) model using the Navy Coupled Ocean Data Assimilation (NCODA) as described by Cummings (2005) (Souza et al, 2020). The HYCOM-NCODA product uses a multi-variate optimal interpolation scheme to assimilate the satellite altimeter observations, satellite and in situ sea surface temperature(SST) observations, as well as in situ vertical temperature and salinity profiles from XBTs, Argo floats and moored buoys (Souza et al, 2020) (Table 2). HYCOM uses a primitive equation composed of Arakawa C grid with  $1/12^\circ$  horizontal resolution and hybrid coordinate by vertical resolution (서 등, 2013). The hybrid coordinate smoothly reverts to a terrain-following coordinate in shallow coastal regions with 41 vertical layers (Shinoda et al, 2019). HYCOM assimilates in situ salinity profiles without the use of satellite-derived Sea Surface Salinity(SSS) products observed in real time (Cummings and Smedstad, 2014; Metzger et al., 2017), and its performance deteriorates when either no in situ observations are available or in

regions of intense river discharge (Jang et al, 2021; Jang et al, 2022). Multiple data (i.e., in situ temperature and salinity profiles, and remotely sensed SST and altimeter sea surface height anomalies) are assimilated by the NCODA three-dimensional variational data assimilation (3DVAR) technique developed for naval numerical weather prediction (NWP) systems (Cummings and Smedstad, 2014; Jang et al, 2022). The reanalysis data were used from 1994 to 2015 and analysis data were used from 2015 to 2017 because of a comparison of the observation data, which ended in 2018. The analysis data were not used to analyze the relationship between Korea Strait and Tokara Strait during spectrum analysis.

#### **OPEM**

Daily ocean reanalysis data from January 2015 to December 2018 produced by the Ocean Predictability Experiment for Marine Environment (OPEM) conducted by the Korea Institute of Ocean Science and Technology were used (Kim et al, 2021) (Table 2). The OPEM is based on the Modular Ocean Model version 5 developed by the Geophysical Fluid Dynamics Laboratory. Its domain covers the northwestern Pacific (98°E-170°E, 5°N-65°N) including the marginal seas around the Korean Peninsula such as the EJS, the Yellow Sea and East China Seas (Kim et al, 2021). The horizontal domain of the KIOST-OPEM ranges from 98 to 170°E and from 5 to 65°N including the Northwestern Pacific and Korean marginal seas with 1/24° grid size both latitudinally and longitudinally. The vertical grid has 51 layers with varying grid size from 10 m at the surface to 367 m near the bottom (김 등 ,2017).

The surface boundary forcing was calculated from the Korea Meteorological Agency's global atmospheric data set (Hong et al., 2018) using the bulk formula of Large and Yeager (2004) (Kim et al, 2021).



<b>Source</b>	<b>Organization</b>	<b>Period of record</b>	<b>Time interval</b>	<b>Resolution</b>	<b>Unit</b>
Current velocity (ship mounted ADCP)	RIAM, Kyushu University	2004-2019 (17 years)	Daily	Vertically 8 m interval	cm/s
Current velocity (bottom mounted ADCP)	RDI, Naval Research Laboratory	1999-2000(1 year)	30 Mins	Vertically 4 m interval	cm/s
Velocity(Reanalysis data)	CMEMS	1994-2017 (17 years)	Daily	1/12°	m/s
Velocity(Reanalysis data and Analysis data)	HYCOM	1994-2017 (17 years)	3 Hourly	1/12°	m/s

Velocity(Reanalysis data)	OPEM	1994-2015	Daily	1/24°	m/s
Volume transport (ship mounted ADCP)	Kagoshima University	1993-2015	4 Day	Vertically 24 m interval	m/s
Volume transport(tidal gauge)	Kongju National University	1975~2018	Monthly	Station	Sv

Table 2. Data used in this study.

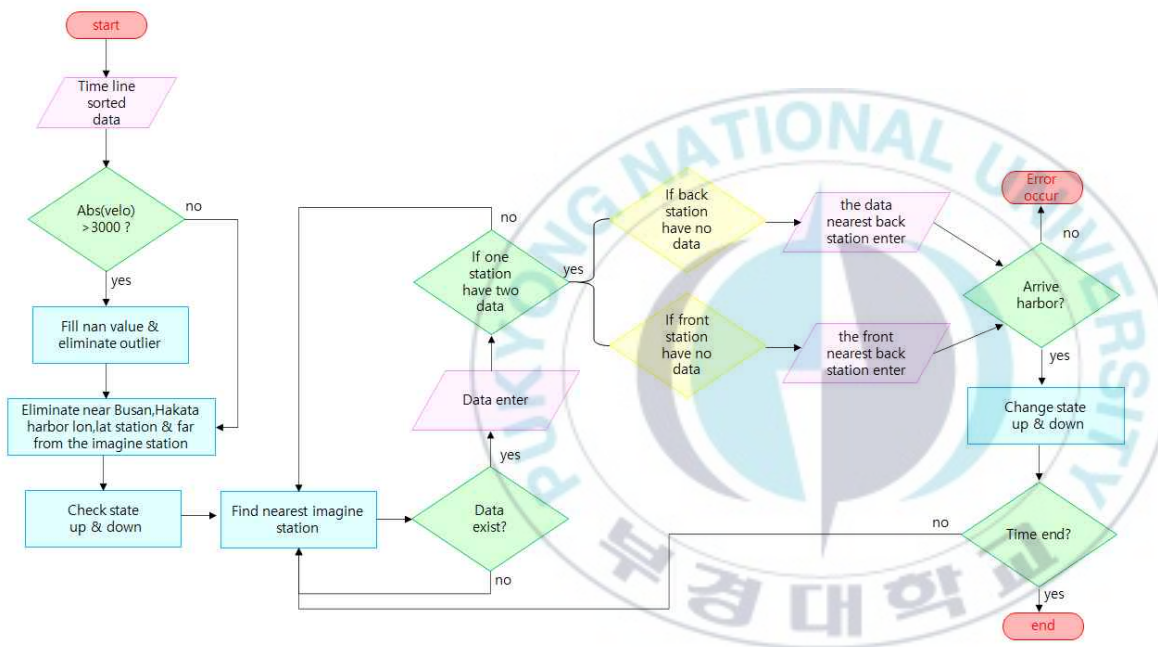


Figure 8. Flow chart how to deal with the ship-mounted ADCP data.

#### 4. CMIP6 Data

As part of the Coupled Climate Model Inter-comparison Project Phase 6 (CMIP6; Eyring et al., 2016), the Scenario Model Inter comparison Project (ScenarioMIP) which defines and coordinates the main set of future climate projections was conducted (O'Neill et al., 2016; 정 등, 2021). The ScenarioMIP experiment produced 21<sup>st</sup> century scenarios based on Shared Socioeconomic Pathways (SSPs) and integrated assessment models(IAMs). Multi-model climate projections represent an essential source of information for mitigation and adaptation decisions (Tebaldi et al, 2021). The SSP-based scenarios address this uncertainty by sampling a larger range of aerosols pathways consistent with the corresponding green house gas(GHG) emissions (Riahi et al., 2017; Tebaldi et al, 2021). The ScenarioMIP design responded to many complex objectives and science questions, among which a high priority was the need to lay the foundation for integrated research across the geophysical, mitigation, impact, adaptation and vulnerability research communities (O'Neill et al., 2020, Tebaldi et al, 2021).

-ScenarioMIP SSP 1-2.6 : target  $2.6 W/m^2$  forced stratospheric-adjusted radiative by the end of the 21st century

-ScenarioMIP SSP 2-4.5 : target  $4.5 W/m^2$  forced stratospheric-adjusted radiative by the end of the 21st century

-ScenarioMIP SSP 5-8.5 : target  $8.5 W/m^2$  forced stratospheric-adjusted radiative by the end of the 21st century

We used the yearly or monthly mean outputs of u,v velocity during the last 10 years of experiments from 2090 to 2100 (Table 3). We used only r1i1p1 from each model to ensure equal weighting in the intermodel analysis. This paper presents outcomes from the 10 CMIP6 models which produced volumes of the Korea Strait better than others.



Number	Institution	Model(s) Ocean	Grid	Model reference(s) and dataset DOIs
1	Korea Institute of Ocean Science and Technology	KIOST-ESM	360 × 200	Pak et al.(2021) <a href="https://doi.org/10.22033/ESGF/CMIP6.1922">https://doi.org/10.22033/ESGF/CMIP6.1922</a> <a href="https://doi.org/10.22033/ESGF/CMIP6.11241">https://doi.org/10.22033/ESGF/CMIP6.11241</a>
2	Max Planck Institute for Meteorology (Germany), also Deutsches Klimarechenzentrum	MPI-ESM1.2-LR	802 × 404	Mauritsen et al.(2019), Mueller et al.(2018) <a href="https://doi.org/10.22033/ESGF/CMIP6.2450">https://doi.org/10.22033/ESGF/CMIP6.2450</a>

	(Germany) and Deutscher Wetterdienst (Germany)			
3	Institut Pierre-Simon Laplace (France)	IPSL-CM6A-LR	362 × 332	Boucher et al.(2020), Hourdin et al.(2020), Lurton et al.(2020) <a href="https://doi.org/10.22033/ES-GF/CMIP6.1532">https://doi.org/10.22033/ES-GF/CMIP6.1532</a>
4	NASA GISS (USA)	GISS-E2.1-G	288 × 180	Kelley et al.(2020), Miller et al.(2021) <a href="https://doi.org/10.22033/ES-GF/CMIP6.2074">https://doi.org/10.22033/ES-GF/CMIP6.2074</a>

5	Met Office Hadley Center (UK)	HadGEM3-GC31 -LL	360 × 330	Sellar et al.(2019), Kuhlbrodt et al.(2018), Williams et al.(2017) <a href="https://doi.org/10.22033/ESGF/CMIP6.1567">https://doi.org/10.22033/ESGF/CMIP6.1567</a> <a href="https://doi.org/10.22033/ESGF/CMIP6.10845">https://doi.org/10.22033/ESGF/CMIP6.10845</a>
6	CNRM-CERFACS (France)	CNRM-ESM2.1	362 × 294	Roehrig et al.(2020); Michou et al.(2020); Voldoire et al.(2019); Seferian et al.(2020) <a href="https://doi.org/10.22033/ESGF/CMIP6.4191">https://doi.org/10.22033/ESGF/CMIP6.4191</a>

				<a href="https://doi.org/10.22033/ESGF/CMIP6.4197">https://doi.org/10.22033/ESGF/CMIP6.4197</a> <a href="https://doi.org/10.22033/ESGF/CMIP6.4198">https://doi.org/10.22033/ESGF/CMIP6.4198</a>
7	CSIRO-ARCCSS (Australia)	ACCESS-CM2	360 × 300	Bi et al.(2020) <a href="https://doi.org/10.22033/ESGF/CMIP6.2285">https://doi.org/10.22033/ESGF/CMIP6.2285</a>
8	Meteorological Research Institute (Japan)	MRI-ESM2.0	360 × 363	Yukimoto et al.(2019) <a href="https://doi.org/10.22033/ESGF/CMIP6.638">https://doi.org/10.22033/ESGF/CMIP6.638</a>
9	Beijing Climate Center (China)	BCC-CSM2-MR	360 × 232	Wu et al.(2019), Xin et al.(2019)

				<a href="https://doi.org/10.22033/ES-GF/CMIP6.1732">https://doi.org/10.22033/ES-GF/CMIP6.1732</a>
10	Nanjing University of Information Science and Technology (China)	NESM3	362 × 292	Cao et al.(2018) <a href="https://doi.org/10.22033/ES-GF/CMIP6.2027">https://doi.org/10.22033/ES-GF/CMIP6.2027</a>

Table 3. Modeling centers and their model(s) used for this study with ocean grid and DOIs.

## 5. Phase Spectrum

The phase spectrum shows the phases of the frequency components of bivariate time series  $x$ . If the time series have same frequency, but different amplitudes and phase, it is written as

$$x_k(t) = A_k \cos(2\pi f_0 t + \phi_k), k = 1, 2$$

$x(t)$  : bivariate time series

$A$  : amplitudes

$\phi$  : phase

Thus, the sample cross-spectra of the two series is

$$S_{12} = \frac{1}{T} [X_1^*(f) X_2(f)]$$

where  $X_1^*$  is the complex conjugate of  $X_1$ . From this expression, the cross amplitude function is written as

$$S_{12}(f) \rightarrow \frac{A_1 A_2}{T} [e^{-i(\phi_2 - \phi_1)\delta(f + f_0)} + e^{-i(\phi_2 - \phi_1)\delta(f - f_0)}]$$

The phase difference,  $(\phi_2 - \phi_1)$  in the above expression determines the lead (or lag) of one cosine oscillation relative to the other for a given frequency,  $f$  and the length of each record,  $T = N\Delta t$  (Thomson and Emery, 2014, p506-508).

## 6. Coherence Spectrum (Coherency)

It is one of spectral analysis which is used to partition the variance of a time series so that it expresses the relation between two time series  $x_1(t)$  and  $x_2(t)$ . It is used to analyze lagged regression in the frequency domain.

$$r_{12}^2(f_k) = \frac{|S_{12}(f_k)|^2}{S_{11}(f_k)S_{22}(f_k)}$$

*r*: coherence

*S*: cross spectra

*f*: frequency



### III. Results

#### 1. The volume transport of Korea Strait

Figure 14 provides a sectional view of climatology mean cross-sectional velocity of Korea Strait based on ship-mounted ADCP. The yearly mean velocities of the cross section in Korea Strait are shown in Figure 12 and Figure 13. The mean current within Korea Strait exhibits two types of flow: a northward flow and a southward flow near Tsushima Island. The southward flow is the countercurrent downstream of the Tsushima Island (Takikawa et al, 2005). The countercurrent tends to be intensified in summer and weakened in winter (Figure 14). It was relatively weak in 2004, 2005, 2009, 2010 and 2017.

The Korea Strait Bottom Cold Water(KSBCW) showed the first maximum southwestward bottom cold water in August/September and secondary maximum in December/January (Kim et al, 2006). As seen Figure 14, the maximum southwestward water in June, July, and August was observed. The cause of the maximum southwestward current in August is due to the maximum baroclinic component (Kim et al, 2006). Indeed, the minimum southwestward bottom water in December/January was observed (Figure 14). The barotropic response dominates the temporal variation of the KSBCW in winter as the vertical stratification weakens (Kim et al, 2006). The North Korean Cold Current (NKCC) might be associated with the maximum

baroclinic bottom current in the Korea Strait in summer (Kim et al, 2006).

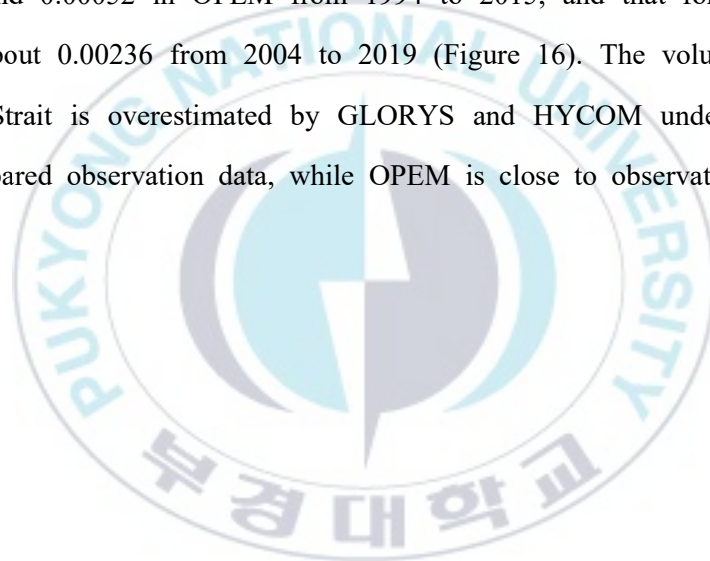
The current in the western channel in 18m is relatively stronger than the current in the eastern channel (Figure 9, Figure 10 and Figure 11). The current in 18m presents maxima of 0.49 m/s in October and 0.28 m/s in the western channel and eastern channel, respectively. Indeed, the current in 18m presents minima of 0.31 m/s in May and 0.18 m/s in January, in the western channel and eastern channel, respectively. Furthermore, the current core in western channel is stronger than the core in the eastern channel (Figure 12, Figure 13 and Figure 14).

Monthly averaged volume transport through Korea Strait across the Camellia line from July, 2004 to December, 2019 are shown in Figure 15 with previous research by Shin et al.(2022) from tidal gauge by KHOA. The yearly volume transport can be seen in Table 4. The average volume transport in Korea Strait over the observation period (about 16 years) is 2.62 Sv. The transports in western channel and eastern channel are 1.30 and 1.32 Sv, respectively. Shin et al.(2022) showed that 2.61-2.64 Sv in total volume transport, and 1.50-1.53 Sv in the western channel, and 1.10-1.11 Sv in the eastern channel.

The magnitude of the velocity was larger in the western channel, but the total transport volume was similar because the width of the eastern channel was larger. The total volume transport in Korea Strait has a maximum value of 3.01 Sv in 2010 and minimum value of 2.15 Sv in 2004. Considering that observation in 2004 was not the yearly data, the minimum volume transport is 2008 of 2.26 Sv. The volume transport in 2010 is the highest in this study on the contrary the volume transport in 2013 by Shin et al.(2022) was the

highest.

We compared the volume transports of Korea Strait from the reanalysis data and observation data from ADCP in time series (Figure 16). The monthly volume transport in reanalysis data time-series have been constructed using current data. It showed that the trend of volume transport in Korea Strait has increased both reanalysis data and observation data. The slope for each data are 0.0004 in GLORYS from 1994 to 2018, 0.00031 in HYCOM from 1994 to 2018, and 0.00052 in OPEM from 1994 to 2015, and that for observation data are about 0.00236 from 2004 to 2019 (Figure 16). The volume transport in Korea Strait is overestimated by GLORYS and HYCOM underestimates it when compared observation data, while OPEM is close to observation.



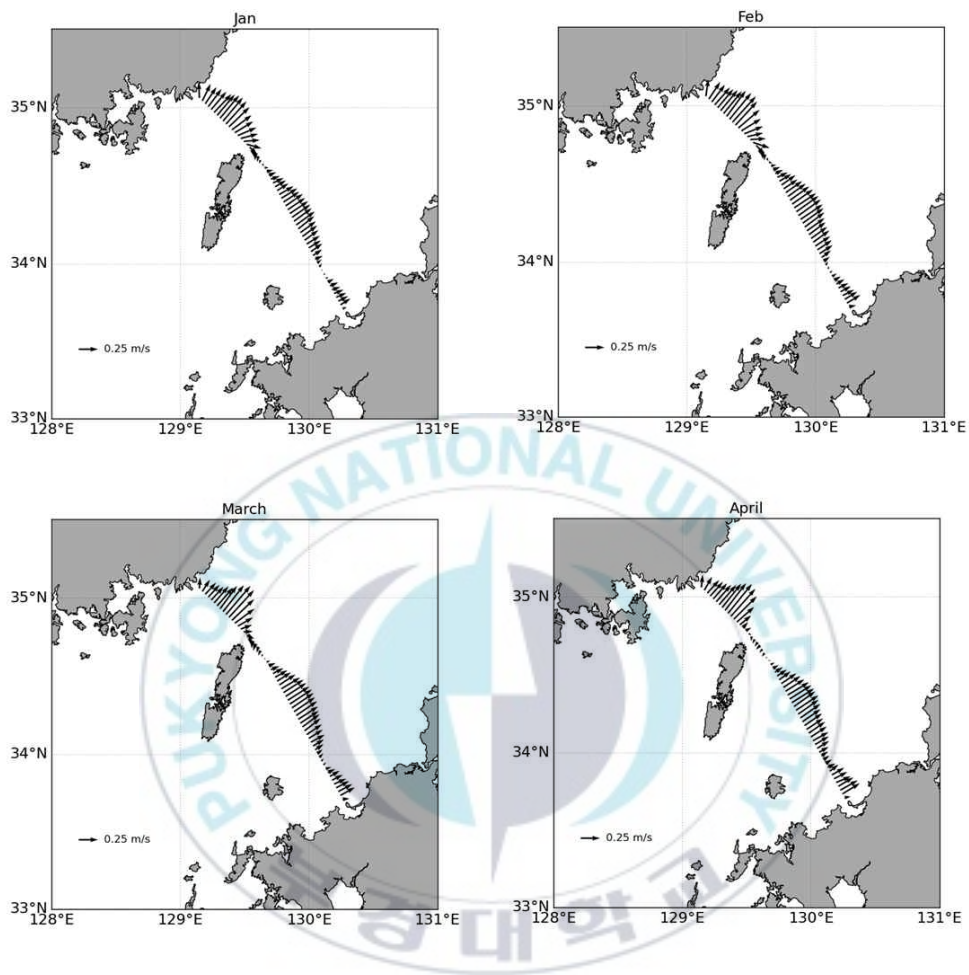


Figure 9. 18m monthly mean velocity from January to April.

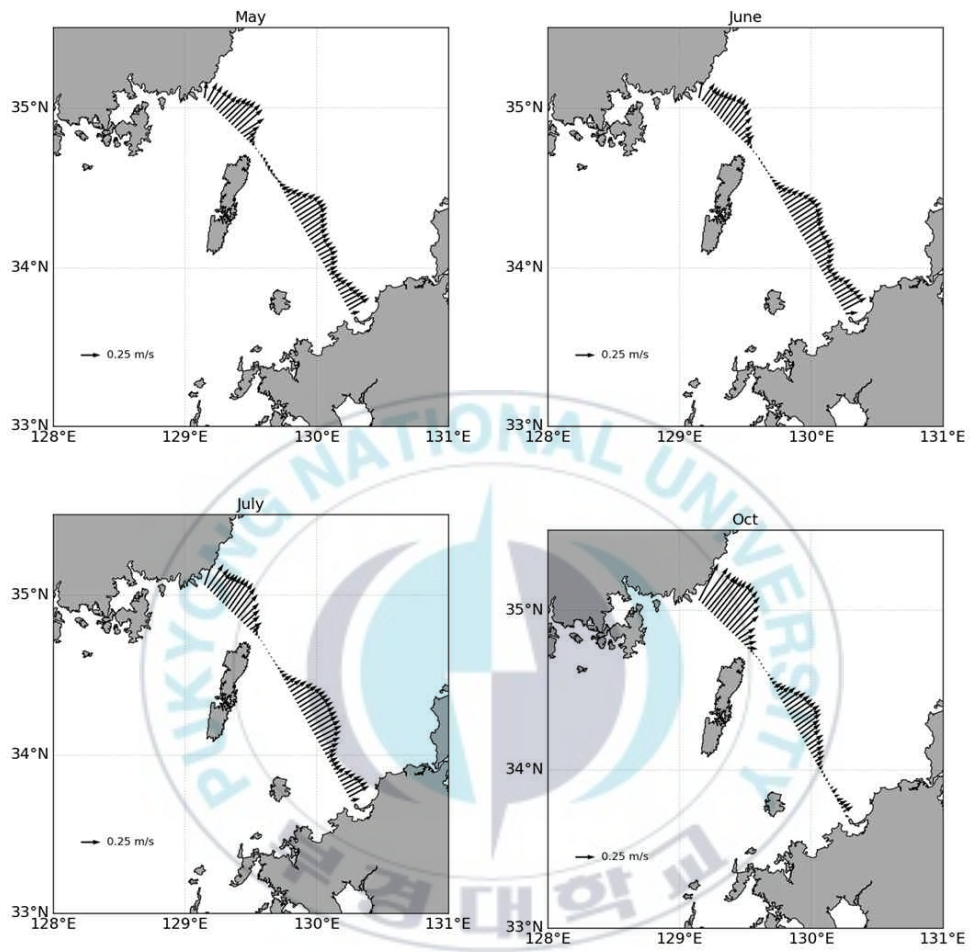


Figure 10. 18m monthly mean velocity from May to August.

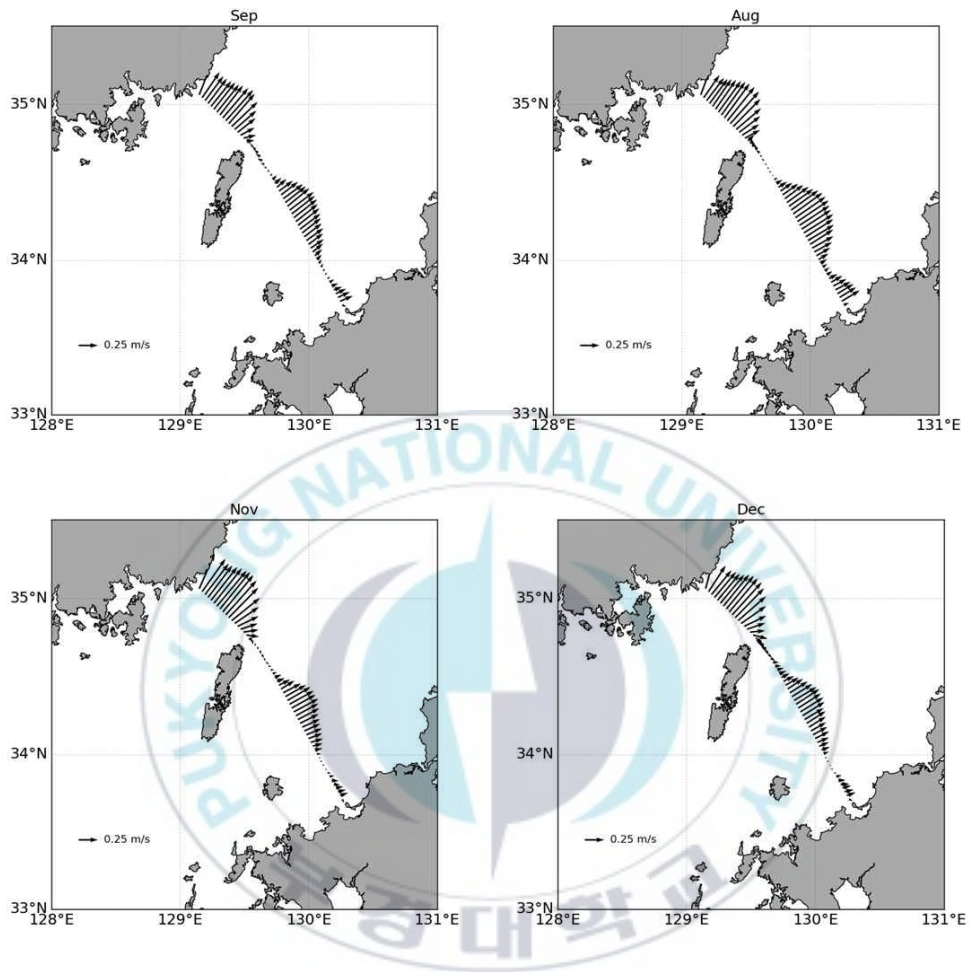


Figure 11. 18m monthly mean velocity from September to December.

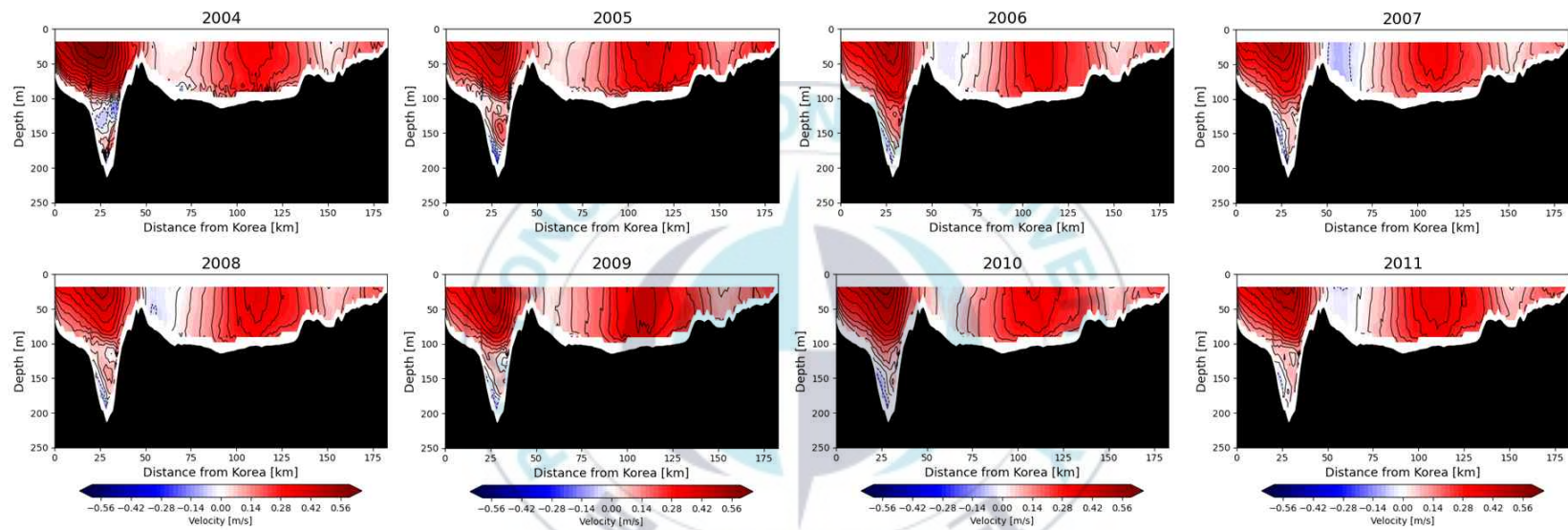


Figure 12. The yearly mean velocity of observation data from 2004 to 2011. Whole year mean data are not available for 2004.

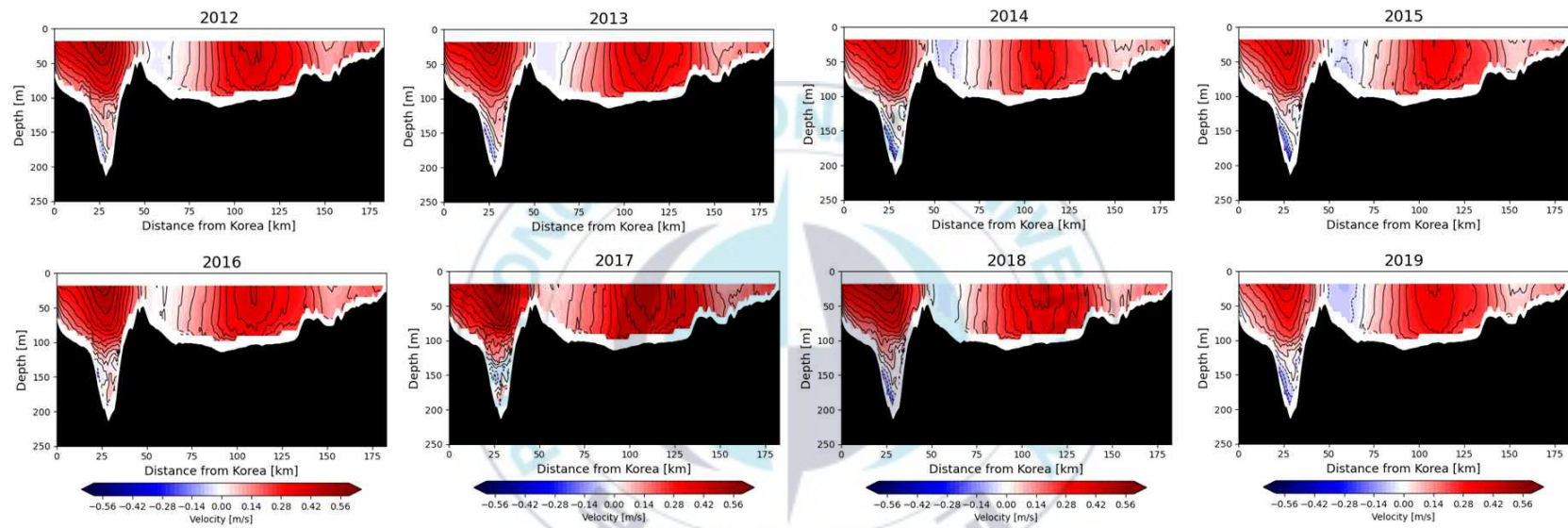


Figure 13. The yearly mean velocity of observation data from 2012 to 2019.

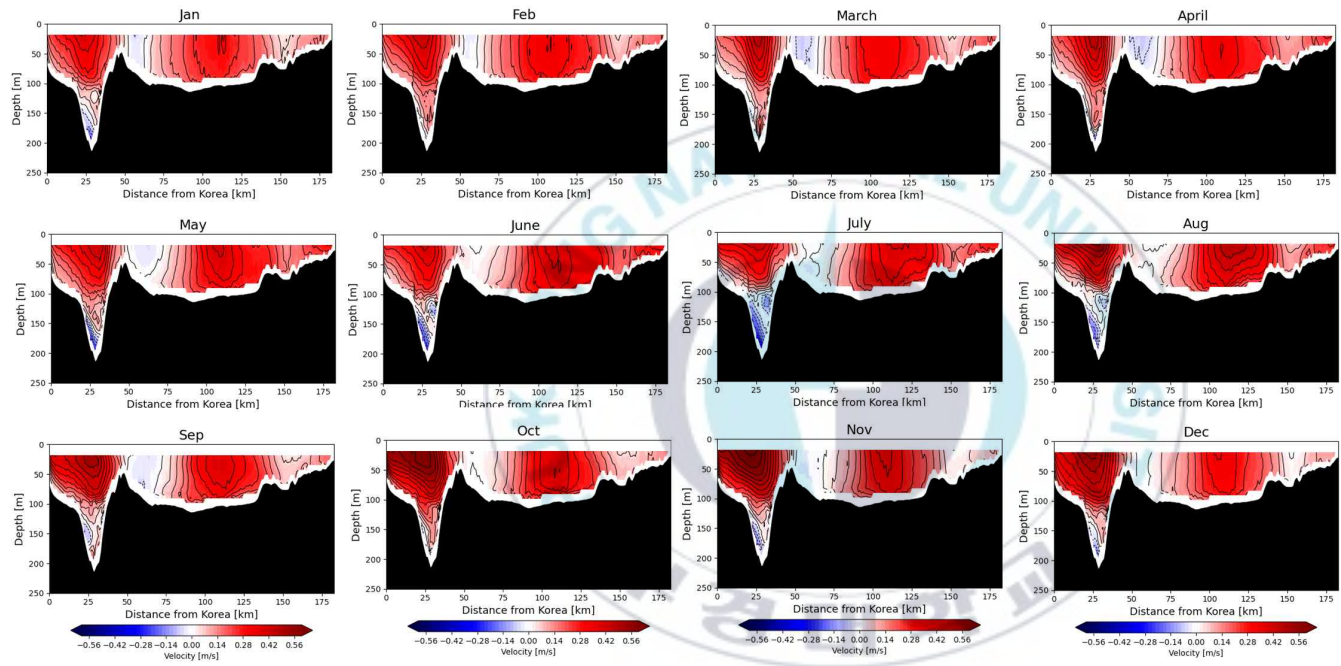


Figure 14. Climatology of observation data in Korea Strait from 2005 to 2019.

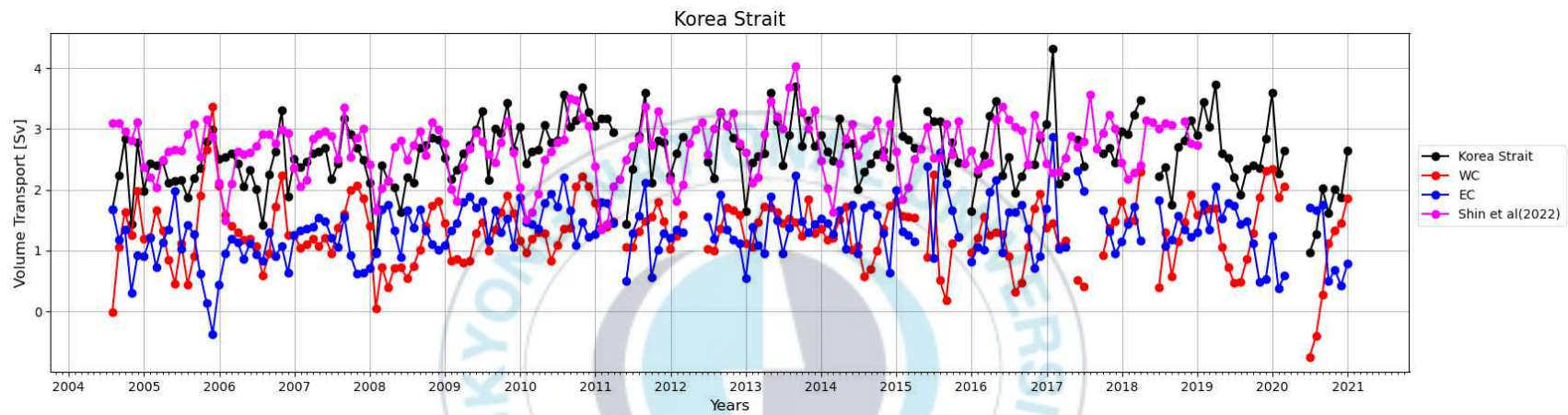


Figure 15. Volume transport in Korea Strait (WC denotes western channel and EC denotes eastern channel of Korea Strait) and volume transport observed by Shin et al. (2022)

Year	Korea Strait	WC	EC
2004	2.15	1.18	0.97
2005	2.38	1.50	0.88
2006	2.33	1.31	1.02
2007	2.56	1.41	1.15
2008	2.26	0.94	1.32
2009	2.78	1.23	1.55
2010	3.01	1.46	1.55
2011	2.68	1.37	1.31
2012	2.63	1.36	1.27
2013	2.90	1.48	1.42
2014	2.66	1.24	1.42
2015	2.71	1.18	1.53
2016	2.60	1.19	1.41
2017	2.72	1.13	1.59
2018	2.76	1.37	1.39
2019	2.75	1.37	1.38

Table 4. The total volume transport and those in the western channel and eastern channel in Korea Strait from 2004 to 2019.

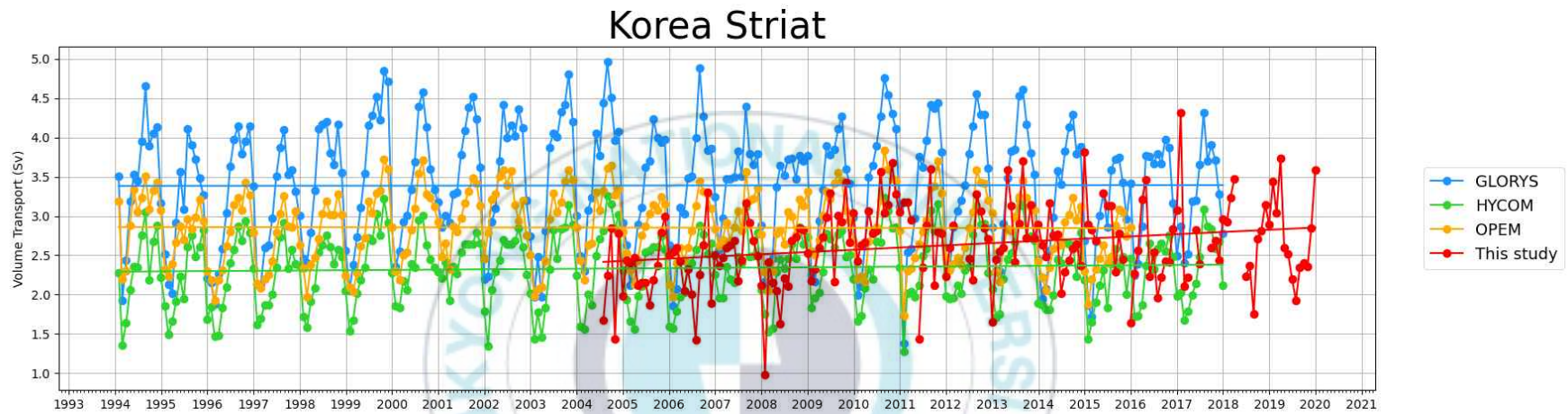


Figure 16. The volume transport of Korea Strait with trend line in reanalysis data and observation data. The blue color denotes GLORYS, lime color denotes HYCOM, yellow color denotes OPEM and the red color express the observation data which is dealt with this study.

## 2. Relationship between Korea Strait and Tokara Strait

The relationship volume transport between Korea Strait and Tokara Strait has been investigated by reanalysis data. Figure 17 shows the yearly volume transport of observation data in Korea Strait and Tokara Strait. The correlation observation between Korea Strait and Tokara Strait of observation from 2005 to 2015 is - 0.76, showing high negative correlation. This implies that there is a relationship between the volume transport in the Korea Strait and the volume transport in the Tokara Strait, such that when one increases, the other decreases, and vice versa. The Kuroshio transport increases from 1975 to 1989, and decreased from 1990 to 2018, showing an opposite tendency to the long-term trend of the TWC transport in Shin et al.(2022). However the region where calculated the Kuroshio transport in Shin et al.(2022) was section along  $137^{\circ}$  that was not the Tokara Strait. Kida et al(2020) also showed that the northward shift in the Kuroshio current makes the increase the Tsushima current.

Figure 18 shows the yearly volume transport both observation from 1993 to 2015 data and reanalysis data from 1994 to 2017 in Tokara Strait. Correlations between observation and reanalysis data in Tokara Strait are 0.75, 0.53, and 0.56 in GLORYS, HCOM and OPEM, respectively. Thus, GLORYS capture the variability of yearly Kuroshio current. Although the correlation in GLORYS is the highest, the volume transport in Tokara Strait is overestimated by GLORYS and HYCOM underestimates it when compared observation data, while OPEM is close to observation.

Figure 20 presents the yearly anomaly volume transport from 2005 to 2017 in observation and from 1994 to 2017 in reanalysis data. When compared to yearly anomaly volume transport of observation, HYCOM presents higher correlation(0.76) than GLORYS(0.72) and OPEM(0.71). Thus, it can be reasonable to use reanalysis data to analyze the region near the Korea Strait.

However, correlation of the monthly volume transport between Korea Strait and Tokara Strait in reanalysis data are 0.27, 0.33 and 0.38 for GLORYS, HYCOM and OPEM, respectively. The monthly correlation between observation and reanalysis data is lower than yearly correlation.

Correlation of yearly anomaly reanalysis data between the Korea Strait and Tokara Strait from 1994 to 2015 are 0.10, -0.41, -0.50 in GLORYS, HYCOM and OPEM, respectively. The correlation between Korea Strait and Tokara Strait from 1994 to 2015 in yearly reanalysis data which does not eliminate climatology are 0.12, -0.38 and -0.50 in GLORYS, HYCOM and OPEM, respectively. HYCOM and OPEM exhibit negative correlation between two straits otherwise GLORYS has positive correlation.

There are volume transports of Korea Strait and Tokara Strait which do not eliminate climatology(Figure 19). There are negative phase in the time series of volume transport in OPEM and the volume transport in GLORYS and HYCOM might appear to change during the long-term(Figure 19). However, the correlation with removed mean value of GLORYS and HYCOM are similar to the correlation with not removed mean value.

There are total monthly volume transport of Korea Strait(top) and Tokara Strait(bottom) with observation data(Figure 21) and monthly volume transport

of each reanalysis data(Figure 22). The correlation between the two straits is negative, but in some years it is positive.



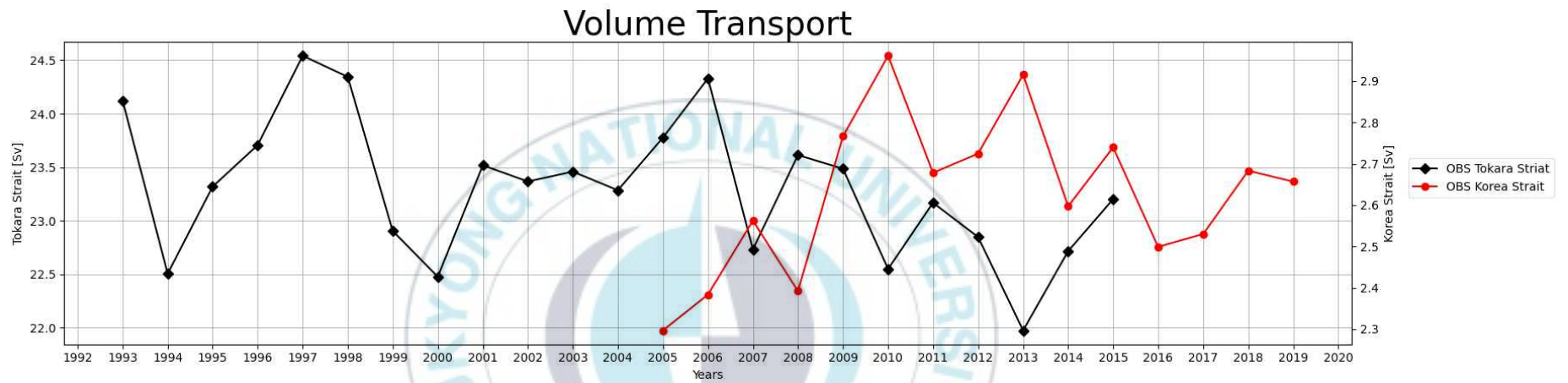


Figure 17. Yearly volume transport of Korea Strait from 2005 to 2019 and Tokara Strait from 1992 to 2015.

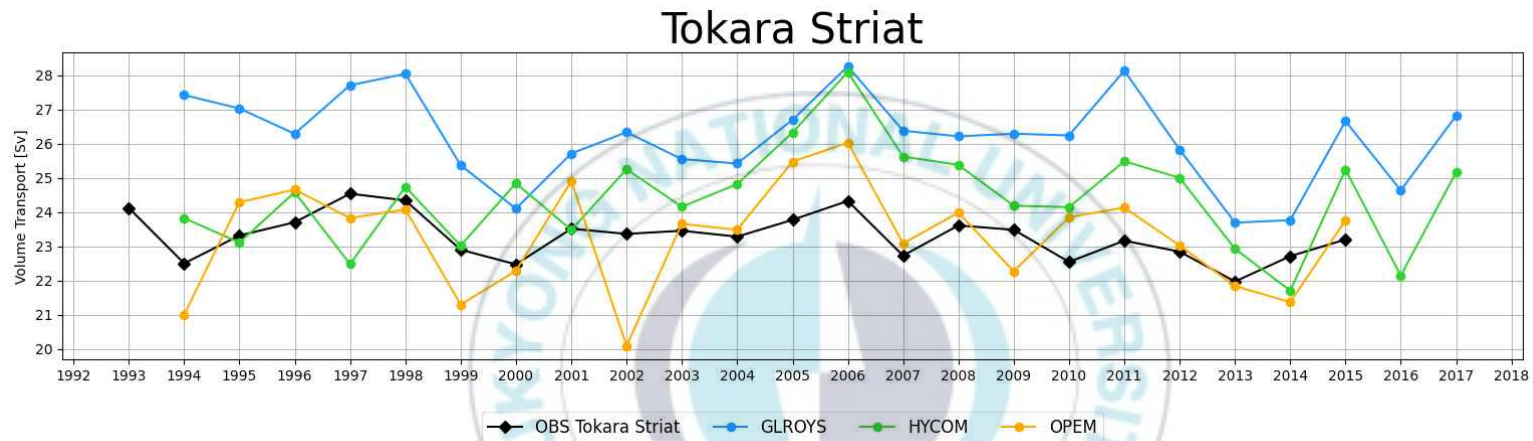


Figure 18. Yearly volume transport of observation data from 1993 to 2015 and reanalysis data from 1994 to 2017 in Tokara Strait.



Figure 19. The volume transport of reanalysis data in Korea Strait and Tokara Strait.

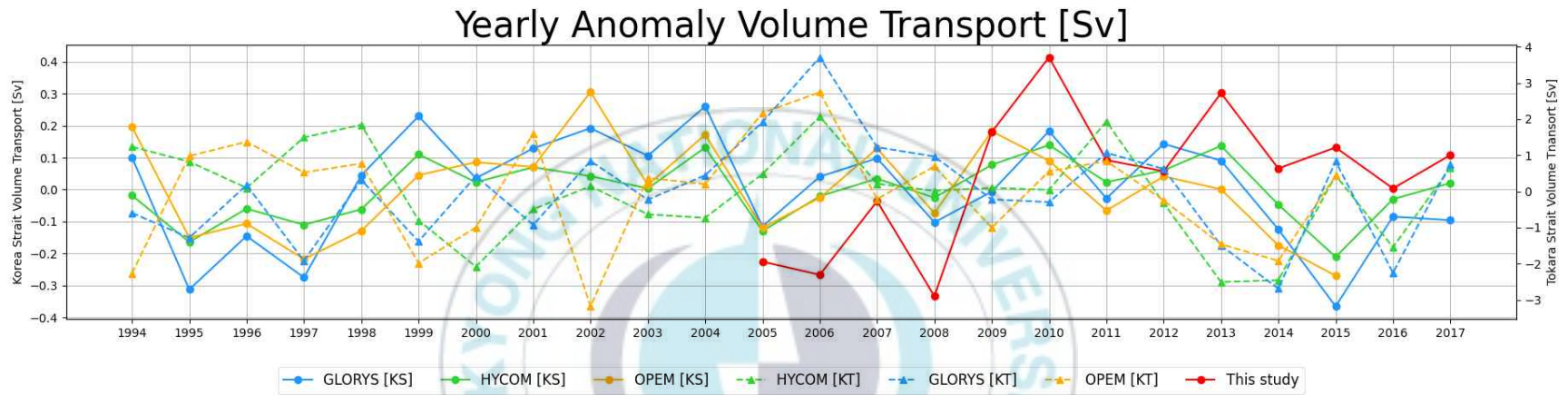


Figure 20. The yearly anomaly volume transport in observation data (red) and reanalysis data. The blue color denotes GLORYS, lime color denotes HYCOM and yellow color denotes OPEM. KS and KT are abbreviations of Korea Strait transport and Kuroshio Current Transport respectively.

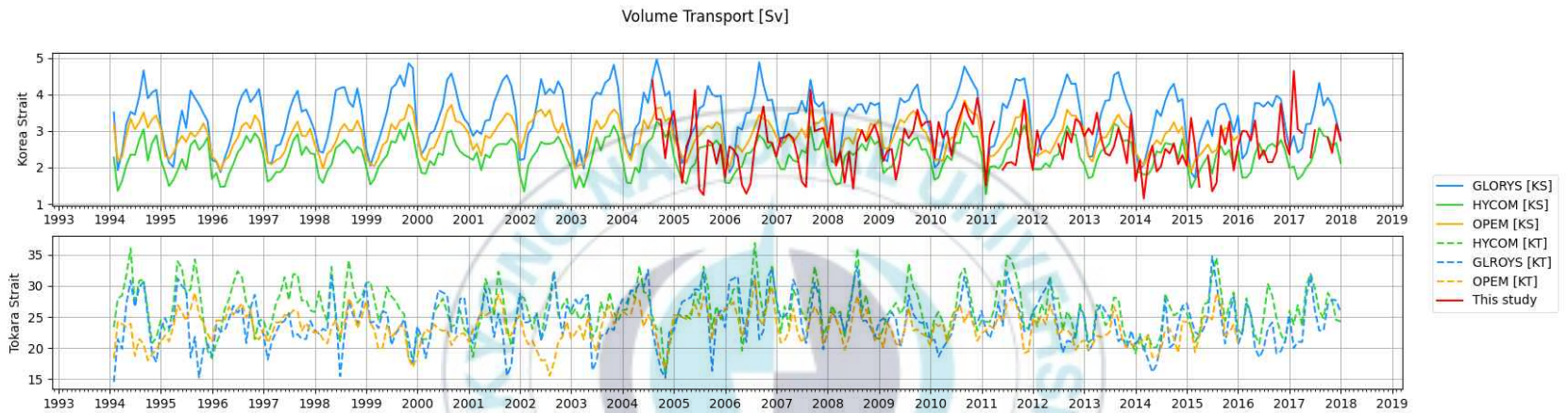


Figure 21. The volume transport in Korea Strait(above) and Tokara Strait(bottom). The blue color denotes GLORYS, lime color denotes HYCOM, yellow color denotes OPEM and red color denotes the observation data which deal with this study.

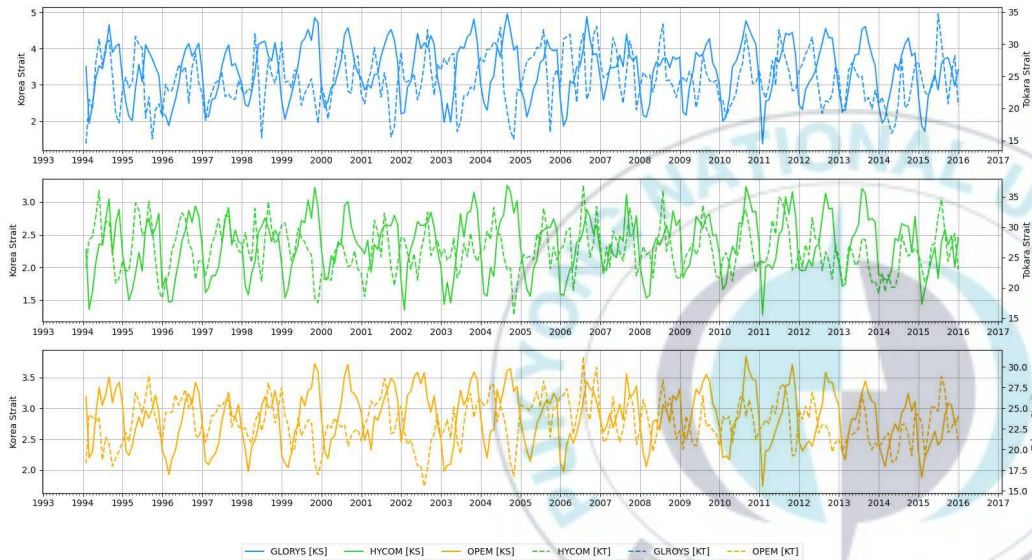


Figure 22. The volume transport of reanalysis time series data. The blue color denotes the GLORYS, green color denotes the HYCOM and the yellow color denotes the OPEM, and the solid and dotted lines denote the volume transports of Korea Strait and Tokara Strait, respectively.

The time series of reanalysis data are used from 1994 to 2015. The coherence was calculated from the frequency domain data of reanalysis data to perform detailed analysis because analysis in time domain has a low correlation, especially monthly lag correlation(Figure 23). The Cross Power Spectral Density is a statistical tool used in signal processing to identify the frequencies at which significant covariance exists between two signals. The cross spectral density has higher density near 0.1 and 0.2 frequencies (Figure 24). In addition, the highest coherence is found near the 0.2 frequency(about 5 months) in monthly reanalysis time series (Figure 25). Thus, significant signal exists near the 0.2 frequency.

The squared spectral coherence, a frequency-domain analog of the squared correlation coefficient, identifies the frequencies at which two variables most strongly covary (Biltoft et al, 2009). Figure 25 presents the coherence spectrum and phase difference of monthly reanalysis data with 95% confidence level. Effective record length is the number of data points available for fft computation. It is found by dividing the total record length ( $t$ ) by the transform size ( $nfft$ ), rounding down to the nearest integer, and multiplying the result by  $nfft$  (Biltoft et al, 2009). There is a significant coherence for  $nfft=60$  that GLORYS and OPEM exhibit 0.796 and 0.791 each near 0.2 frequency and HYCOM exhibits 0.891 near 0.18 frequency. The significance occurs for periods of around 5 months. The phase difference of significant coherence for the volume transport are  $-172.98^\circ$ ,  $-176.78^\circ$  and  $-147.39^\circ$  in GLORYS, HYCOM and OPEM, respectively.

The negative coherent peak can explain Tokara Strait leads Korea Straits at

around the 5 month period. The lead and lag depends on the sequence. In this study, as the volume transport is based on Korea Strait, the negative coherency can explain that Tokara Strait leads the Korea Strait. As the time lag induced by  $(\text{time lag}/\text{period}) \times 360 = \text{phase lag}$ , the time lags are 2.38, 2.44 and 2.04 months in GLORYS, HYCOM and OPEM, respectively. There is a negative correlation between two strait in observation yearly data. Even though the coherence at 1 year in GROLYS is under 95% confidence level, phase differences in the coherence spectrum are  $-159.059$  and  $-130.304$  respectively for periods 5.3 months and 4.33 months in HYCOM and OPEM, respectively. There is a lead-lag relationship between Korea Strait and Tokara Strait. Tokara Strait could leads Korea Strait by 5.3 month in HYCOM and 4.33 month in OPEM.



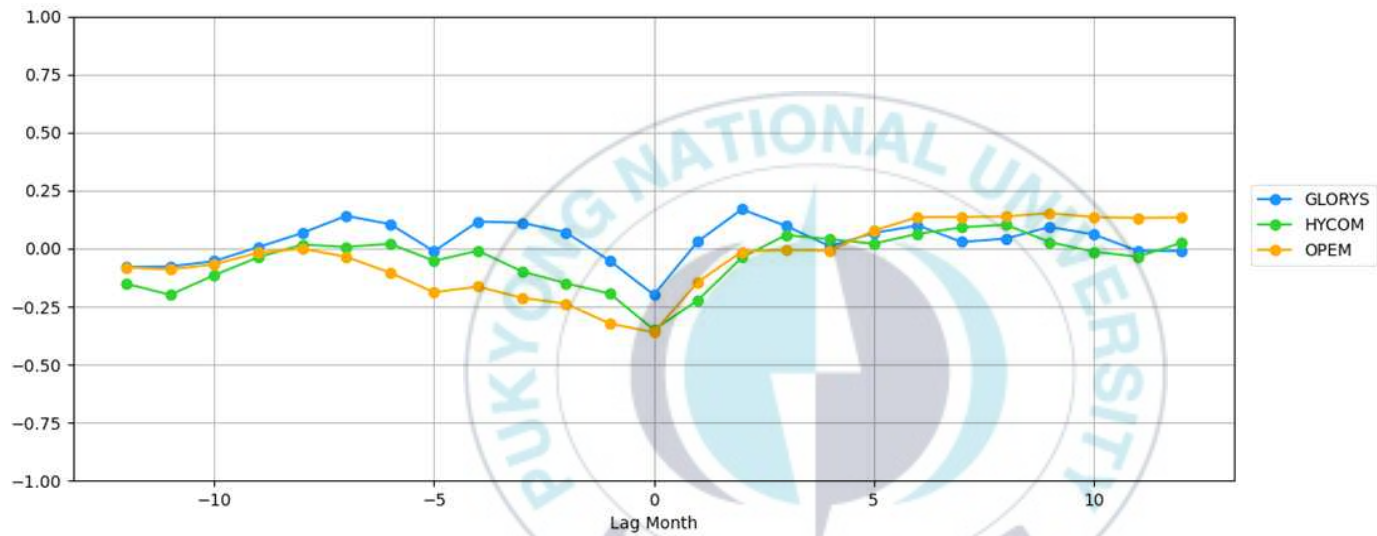


Figure 23. Monthly lag correlation in GLORYS(blue), HYCOM(lime) and OPEM(yellow).

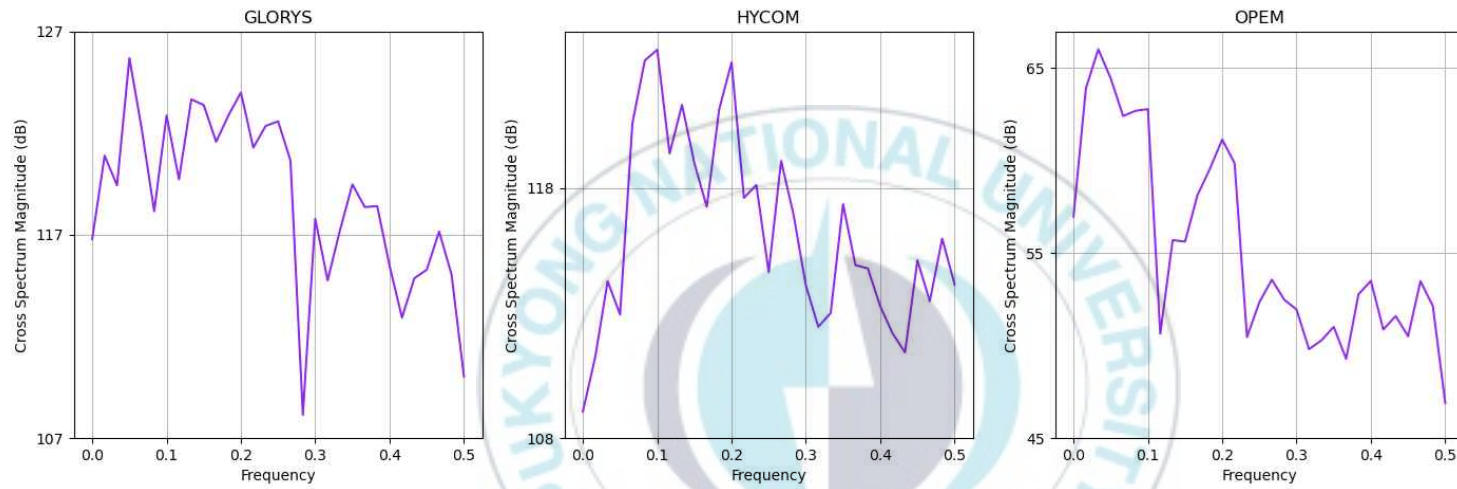


Figure 24. Cross spectral density using monthly reanalysis data.

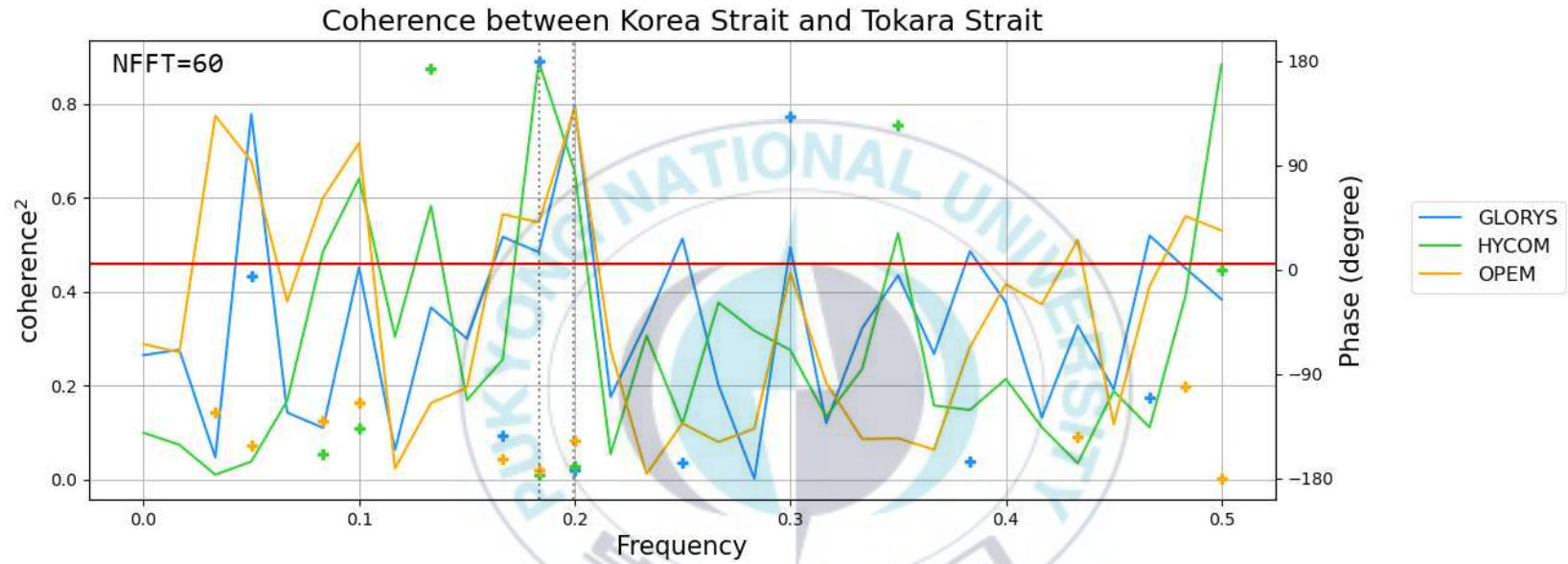


Figure 25. Coherence and phase (+) between monthly time series in GLORYS (blue), HYCOM (lime), and OPEM (yellow). The gray vertical lines show the highest coherence vector in each model, and red horizontal line denotes the 95% confidence level in coherence spectrum.

### 3. CMIP6

In response to the global warming, the Kuroshio current is expected to be strengthened as the Hadley Circulation poleward shift in scenarioMIP 1-2.6, 2-4.5 and 5-8.5 in CMIP6 with increasing volume transport through Korea Strait in 정 등(2021). 정 등(2021) focused on the relationship between volume transport and Kuroshio current poleward and used 4 CMIP6 models to analyze the Korea Strait. Thus, we used more CMIP6 models than 정 등(2021) and attempted to find out how the volume transport changes both in Korea Strait and Tokara Strait in the future.

Figure 26 and Figure 27 show the volume transport in Korea Strait and Tokara Strait during future period(2090-2100) in SSP1-2.6, SSP2-4.5 and SSP5-8.5, respectively and black color denotes ensemble mean which is the sum of 10 models. The slope of volume transport in Korea Strait are  $-0.0010$ ,  $0.0009$ ,  $0.0005$  in SSP1-2.6, SSP2-4.5 and SSP5-8.5 respectively. The ensemble mean of volume transport in Korea Strait is 1.92, 1.94 and 2.16 in SSP1-2.6, SSP2-4.5 and SSP5-8.5, respectively. As the same way, the slope of volume transport in Tokara Strait is  $-0.0008$ ,  $0.0017$  and  $-0.0002$  in SSP1-2.6, SSP2-4.5 and SSP5-8.5 respectively. The ensemble mean of volume transport in Tokara Strait is 6.94, 6.81 and 6.69 in SSP1-2.6, SSP2-4.5 and SSP5-8.5 respectively (Table 5). Considering the difficulties in identifying the region of the two strait, ensemble volume transport is more important than the trend. The volume transports of Korea Strait and Tokara Strait are relatively low when compared with the observations by Figure 17.

As the radiative forcing due to the increase in greenhouse gases becomes stronger, the Kuroshio current showed to be strengthened in most models in 정 등(2021). The volume transport in Korea Strait expected increase as global warming becomes more severe. Furthermore, the volume transport might decrease in Tokara Strait as the amount of carbon dioxide increased further. That is, volume transport of Korea Strait and Tokara Strait have opposite tendency. Zero windstress curl in North Pacific is considered the boundary between the subtropical and polar circulations and is associated with changes in the Hadley circulation.

The poleward expansion of the Hadley circulation may have important impacts on northwest Pacific. The increase in volume transport of Korea Strait and the decrease in volume transport of Tokara Strait might be caused by poleward of Hadley circulation. The time series of zero windstress curl latitude of CMIP6 and ERA5 in mid-latitude of the north Pacific have increased(정 등, 2021) (Figure 29). The ensemble mean of middle-latitude of north Pacific ocean are  $44.26^{\circ} N$ ,  $44.28^{\circ} N$ , and  $44.71^{\circ} N$  in each scenario which means that Hadley circulation might increase in Figure 29. Although the poleward of Hadley circulation does not coincide with the poleward of Kuroshio current, there are closely connected. The poleward mean latitude in the Hadley circulation is consistent with the poleward of the position of the Kuroshio Extension. Regions where the Kuroshio current became stronger appeared similar to regions in most of CMIP6 where SST rises significantly in Figure 28. It also can be thought that the more warm Tsushima current flows into the Korea Strait (Figure 30). Changes in the Kuroshio current are expected to

contribute to a greater increase in SST around the Korean Peninsula than the global average by bringing about changes in the heat transport in the northwest Pacific. Kuroshio current axis poleward makes the volume transport of Korea Strait increased with decreasing the volume transport of Tokara Strait. Even though the slope of fitting line is not decreasing in SSP2-4.5 in Tokara Strait, the ensemble mean value is greater than that in SSP5-8.5 and smaller than that in SSP1-2.6.



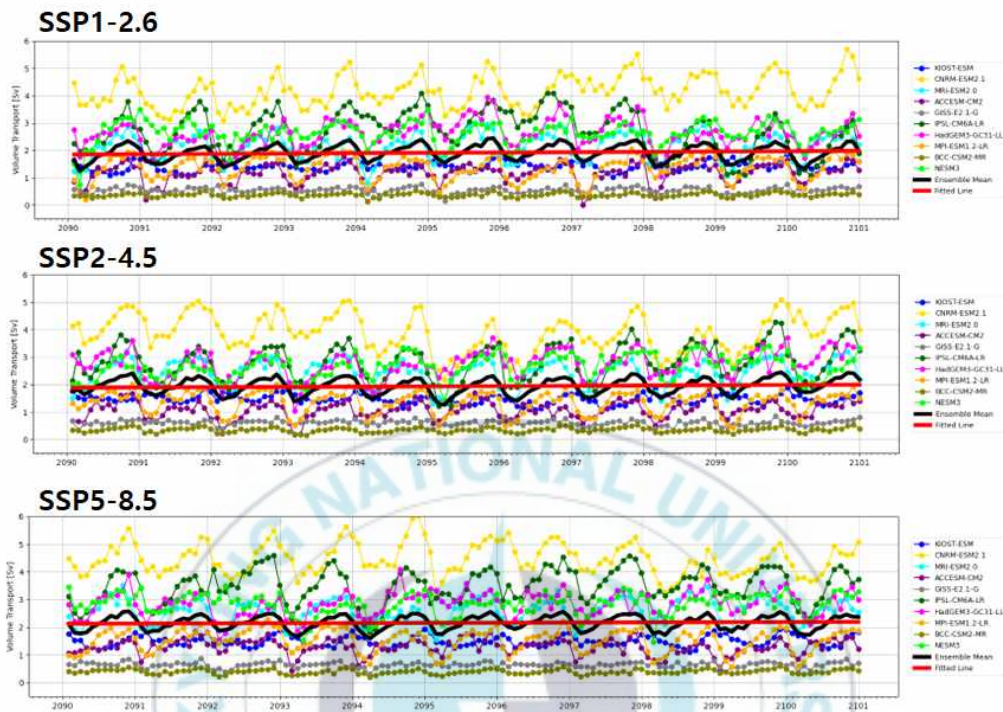


Figure 26. Volume transport of Korea Strait from 2090 to 2100.

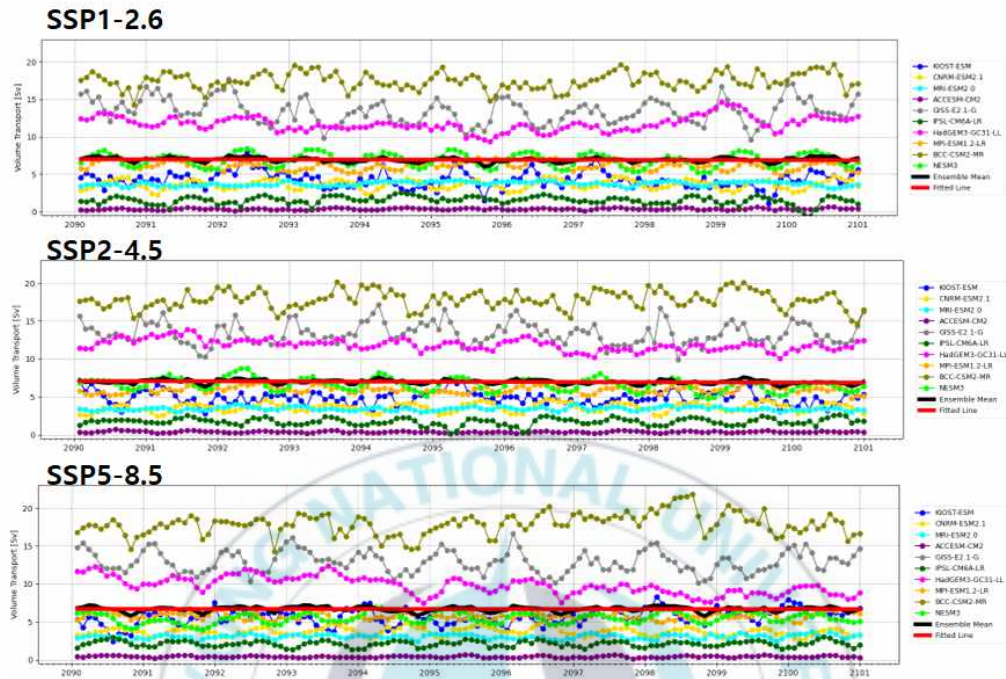


Figure 27. Volume transport of Tokara Strait from 2090 to 2100.

	SSP1-2.6	SSP2-4.5	SSP5-8.5
Korea Strait	1.92	1.94	2.16
Tokara Strait	6.94	6.81	6.69

Table 5. Ensemble mean of volume transport of each scenario in Korea Strait and Tokara Strait from 2090 to 2100.

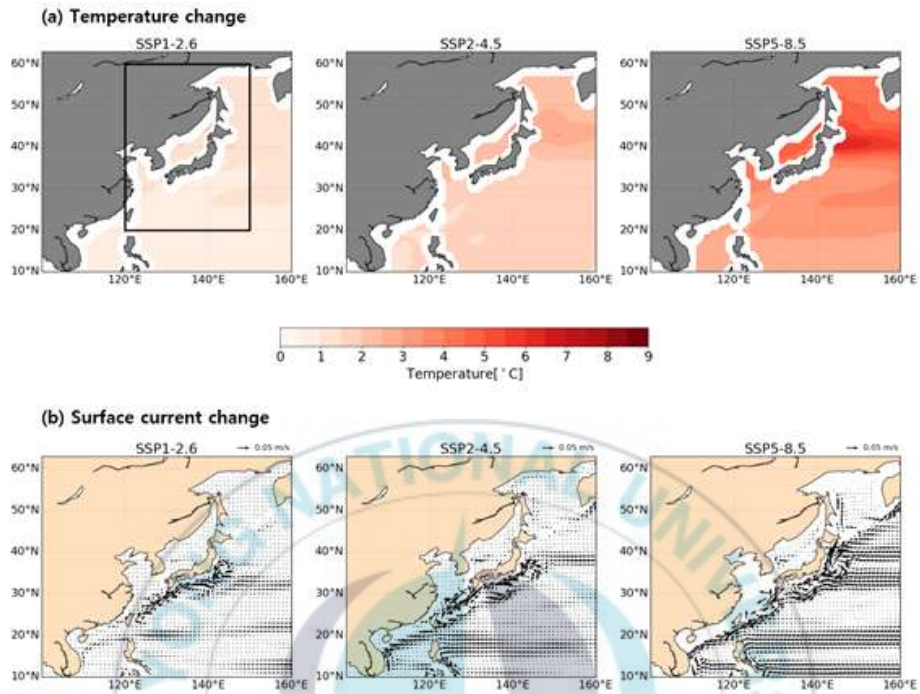


Figure 28. Sea Surface Temperature (a) and surface current (b) change (2091-2100) according to ScenarioMIPs from each historical simulations (2005-2014) from ensemble mean of 9 models (KIOST-ESM, MRI-ESM2.0, INM-CM4.8, INM-CM5.0, IPSL-CM6A-LR, GISS-E2.1-G, EC-Earth3, CNRM-ESM2.1, ACCESS-CM2). Left, middle, right panels denote SSP1-2.6, SSP2-4.5, SSP5-8.5 respectively (정 등, 2021).

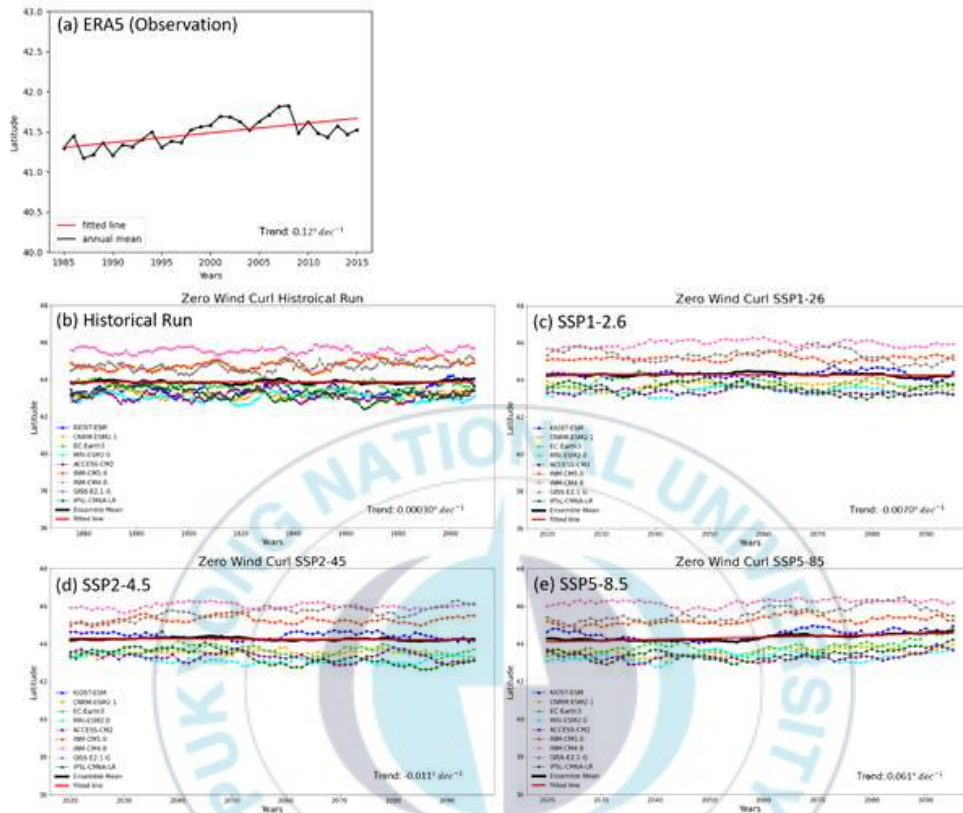


Figure 29. Time series of zero windstress curl latitude in mid-latitude of the North Pacific (10-year running average) from ERA5 observation and ScenarioMIPs of 9 models. (a) ERA5 reanalysis (observation), (b) ScenarioMIP SSP1-2.6, (c) ScenarioMIP SSP2-4.5, (d) ScenarioMIP SSP5-8.5 (정 등, 2021).

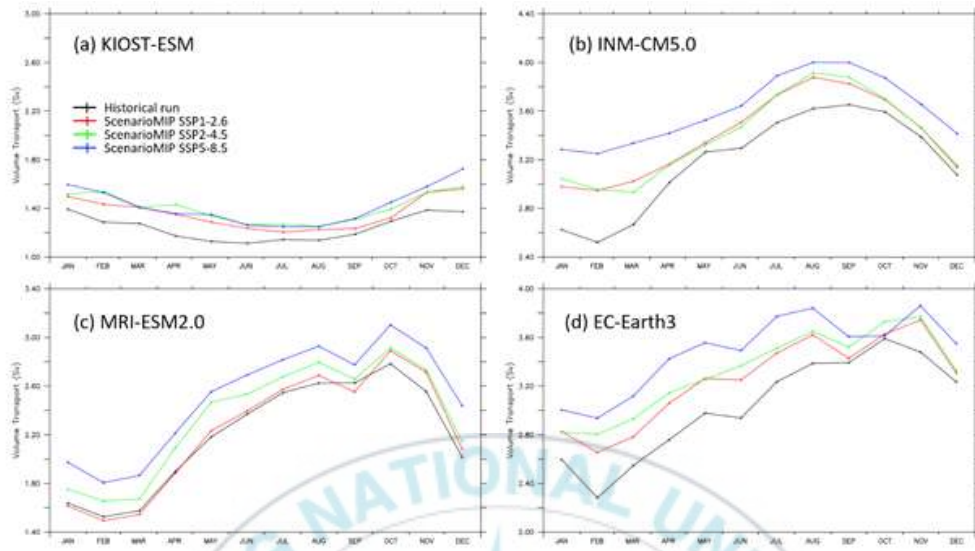


Figure 30. Volume transport of the Tsushima Warm Current through the Korea Strait for historical simulations (2005-2014) and ScenarioMIP simulations (2091-2100) (정 등,2021).

## IV. Conclusion and Discussion

There is a long-term observation data set collected by ship-mounted ADCP from July, 2004 to December, 2019. The velocity of surface layer and bottom layer are contaminated by scattering effect so that layers are needed to be extrapolation. The use of gradient extrapolation in the bottom layer and same value in the first bin. The average volume transport through the Korea Strait over 16 years was 2.62 Sv. The transport through the western and eastern channels were 1.30 and 1.32 Sv respectively. The total volume transport through the Korea Strait showed a maximum of 3.01 Sv in 2010 and a minimum of 2.15 Sv in 2004. The ship-mounted ADCP were considered well processed, as it shows the presence of the countercurrent near Tsushima and the Korea Strait Bottom Cold Water in the summer season.

The trend of reanalysis data and observation data in Korea Strait have increasing trend. That implies volume transport in Korea Strait might increase when Kuroshio current is poleward to make Tsushima current more flow in Korea Strait.

Results from several recent studies have suggested a negative correlation between the volume transport through the Korea Strait and the Tokara Strait. This study found that when analyzing the observed volume transport data for the Korea Strait and Tokara Strait on a yearly basis, there was a high negative correlation of  $-0.76$ . It can be explained when volume transport in Korea Strait increases, the volume transport in Tokara Strait decreases, and

vice versa. This study expected a negative correlation between the volume transport through the Korea Strait and the Tokara Strait in reanalysis data. However, when analyzing the monthly data, the correlation between the two straits in the reanalysis data was found to be low. Even if the correlation is the lowest at zero lag, there was no significant negative lag correlation between the two straits from 1994 to 2015.

This study found no significant results in the time domain, so we tried to analyze the data using spectrum analysis in the frequency domain. When analyzing the cross-spectrum density of the three reanalysis data sets, it was found that the density was high at the 0.2 frequency. The results of the analysis revealed a negative phase difference between the Korea Strait and the Tokara Strait at the 0.2 frequency. Thus, it is reasonable to assume that Tokara Strait about 2 month leads Korea Strait by 5 month.

In comparing the reanalysis data with the observation data, it was found that GLORYS showed a high correlation in both the Korea Strait and the Tokara Strait. However, the yearly volume transport in Korea Strait is overestimated by GLORYS and HYCOM underestimates it when compared observation data, while OPEM is close to observation.

This study attempted to analyze the volume transport in Korea Strait and Tokara Strait in the future climate with CMIP6 models. The results suggest that the volume transport through the Korea Strait expects to increase, while the volume transport through the Tokara Strait expects decrease in the future climate. This is attributed to the poleward movement of the Hadley circulation, which causes the Kuroshio current to move poleward, and the increased flow

of the warm Tsushima current, a branch of the Kuroshio current, into the Korea Strait. The results suggest that as the Hadley circulation expands northward due to global warming, the warming trend in the mid-latitudes, including the Korean Peninsula, expects to be accelerated. However, it is difficult to analyze the correlation of volume transport between Korea Strait and the Tokara Strait because of the difficulty in identifying the region of the Tokara Strait in the CMIP6 models.



## 대한해협 수송량의 현재와 미래

정수연

부경대학교 대학원 지구환경시스템과학부 해양학전공

### 요약

대한해협을 통과하는 대마난류는 동해로 열, 염분, 운동량 등을 수송하고 있어, 대한해협 수송량을 정확하게 파악하는 것은 중요하다. 대마난류는 쿠로시오 해류의 지류로써 대한해협 수송량 연구를 위해서는 쿠로시오 해류와의 관계를 알아보는 것도 중요하다. 본 연구에서는 ADCP 관측값과 고해상도 재분석자료인 GLORYS, HYCOM, OPEM을 이용해 분석을 진행했다. 일본 하카타와 한국 부산을 왕복하는 여객선인 Camellia 호에 장착된 ADCP로부터 최소자승법을 이용하여 관측선의 경로를 새로 설정하고, 14개 분조를 조화 분해하여 조석 성분이 제거된 해류 자료를 얻을 수 있었다. 또한, 관측이 어려운 표층과 바닥층의 해류를 추정하기 위하여 NRL에서 관측한 ADCP 자료를 이용하여 대한해협에 맞는 외삽 방법을 찾고자 하였다. 바닥층까지 기울기를 내리는 방법이 가장 잘 적

합한 것으로 판단하여 외삽을 수행했고, 표층에서는 첫 층의 관측값을 이용해 외삽하여 대한해협 수송량을 구하였다. 그리하여 Camellia ADCP 자료로부터 대한해협을 통한 대마난류의 평균 수송량을 2.69 Sv 으로, 서수도와 동수도를 통한 수송량을 각각 1.34 Sv, 1.45 Sv으로 추정할 수 있었다.

대한해협 수송량의 시간 변화를 파악하기 위하여 현장 관측값과 재분석 자료를 함께 분석한 결과, 대한해협 수송량은 시간에 따라 증가하는 특징을 보였다. 또한, 대한해협과 쿠로시오 해류와의 관계를 알아보기 위해서, 대한해협과 토카라해협의 상관관계 및 스펙트럼 분석을 수행하였다. 관측자료를 이용하여 계산한 상관관계는 -0.76으로 높게 나타났으며, 재분석자료를 이용하여 스펙트럼 분석을 수행한 결과, 5달 주기에서 토카라해협의 수송량이 대한해협의 수송량을 약 2달 정도 선행하는 것으로 나타났다.

미래 기후에서 대한해협과 쿠로시오 해류와의 관계를 알아보기 위해 10개의 CMIP6 모델 결과를 분석했다. 복사 강제력이 강해지는 시나리오일 수록 쿠로시오 해류가 북상하였으며 2090년에서 2100년 사이의 대한해협 수송량은 증가, 토카라해협 수송량은 감소했다. Zero-바람회전 응력은 해양 및 대기 순환의 경계를 나타내는데, 해들리 순환의 중위도 평균 위도는 지구온난화가 진행될수록 북쪽에 위치하였고, ERA5 자료에서도 과거 30년 동안 북태평양 중위도 해역의 평균 위도가 북쪽으로 이동하는 것을 확인하였다. 해들리 순환의 북상은 쿠로시오 해류의 북상에 영향을 주어 쿠로시오 확장역의 위치가 북상하는 원인으로 해석할 수 있다. 그로 인해 대한해협을 통과하는 대마난류의 수송량은 증가하고, 토카라해협을 통과하는 쿠로시오의 수송량은 줄어드는 것으로 전망된다. 증가하는 대

마난류로 한반도 주변의 해면수온이 상승하고, 이러한 결과는 지구온난화로 인한 한반도 및 북서태평양 주변의 해류와 해면수온에 변화를 줄 것으로 전망된다.



## References

- 김영호, 진현근, 박균도 (2017). Development of the KIOST regional ocean prediction system : OPEM (Ocean Predictability Experiment for Marine environment), GODAE Oceanview DA-TT Workshop, pp.1
- 정수연, 최소현, 김영호 (2021). CMIP6 모형 결과 분석을 통한 북서태평양 해면수온과 해류의 미래변화에 대한 고찰, 한국해양학회지, 4, 291-306.
- 서성봉, 박영규, 박재훈, 이호진, N. Hirose (2013). 고해상도 해양예보모형 HYCOM에 재현된 쓰시마난류, Ocean and Polar Research, 35(2): 135-146.
- 内海, 勇哉 (2018). フェリーADCPデータに基づく対馬海峡流動構造の再解析, Kyushu University Library.
- Andres, M., Park, J. H., Wimbush, M., Zhu, X. H., Nakamura, H., Kim, K., & Chang, K. I. (2009). Manifestation of the Pacific decadal oscillation in the Kuroshio. Geophysical Research Letters, 36(16).
- Bahmani, A., Mueller, F. (2018). Chameleon: Online Clustering of MPI Program Traces. Mauritsen, T., Bader, J., Becker, T., Behrens, J., Bittner, M., Brokopf, R., Brovkin, V., Claussen, M., Crueger, T., Esch, M., Fast, I., Fiedler, S., Fläschner, D., Gayler, V., Giorgetta, M., Goll, D. S.,

Haak, H., Hagemann, S., Hedemann, C., Hohenegger, C., Ilyina, T., Jahns, T., Jimenéz-de-la-Cuesta, D., Jungclaus, J., Kleinen, T., Kloster, S., Kracher, D., Kinne, S., Kleberg, D., Lasslop, G., Kornblueh, L., Marotzke, J., Matei, D., Meraner, K., Mikolajewicz, U., Modali, K., Möbis, B., Müller, W. A., Nabel, J. E. M. S., Nam, C. C. W., Notz, D., Nyawira, S., Paulsen, H., Peters, K., Pincus, R., Pohlmann, H., Pongratz, J., Popp, M., Raddatz, T. J., Rast, S., Redler, R., Reick, C. H., Rohrschneider, T., Schemann, V., Schmidt, H., Schnur, R., Schulzweida, U., Six, K. D., Stein, L., Stemmler, I., Stevens, B., von Storch, J.- S., Tian, F., Voigt, A., Vrese, P., Wieners, K.-H., Wilkenskield, S., Winkler, A., and Roeckner, E. (2019), Developments in the MPI-M Earth System Model version 1.2 (MPI-ESM1.2) and Its Response to Increasing CO<sub>2</sub>, *J. Adv. Model. Earth Syst.*, 11, 998– 1038.

Bi, D., Dix, M., Marsland, S., O'Farrell, S., Sullivan, A., Bodman, R., Law, R., Harman, I., Srbinovsky, J., Rashid, H. A., Dobrohotoff, P., Mackallah, C., Yan, H., Hirst, A., Savita, A., Dias, F. B., Woodhouse, M., Fiedler, R., and Heerdegen, A. (2020). Configuration and spin-up of ACCESS-CM2, the new generation Australian Community Climate and Earth System Simulator Coupled Model, *J. South. Hemisphere Earth Syst. Sci.*, 70, 225–251.

Biltoft, C. A., & Paradyjak, E. R. (2009). Spectral coherence and the statistical significance of turbulent flux computations. *Journal of atmospheric and*

oceanic technology, 26(2), 403-409.

Boucher, O., Servonnat, J., Albright, A., Aumont, O., Balkanski, Y., Bastrikov, V., Bekki, S., Bonnet, R., Bony, S., Bopp, L., Braconnot, P., Brockmann, P., Cadule, P., Caubel, A., Cheruy, F., Codron, F., Cozic, A., Cugnet, D., D'Andrea, F., Davini, P., de Lavergne, C., Denvil, S., Deshayes, J., Devilliers, M., Ducharne, A., Dufresne, J., Dupont, E., Éthé, C., Fairhead, L., Falletti, L., Flavoni, S., Foujols, M., Gardoll, S., Gastineau, G., Ghattas, J., Grandpeix, J., Guenet, B., Guez, L., Guilyardi, E., Guimberteau, M., Hauglustaine, D., Hourdin, F., Idelkadi, A., Joussaume, S., Kageyama, M., Khodri, M., Krinner, G., Lebas, N., Levvasseur, G., Lévy, C., Li, L., Lott, F., Lurton, T., Luysaert, S., Madec, G., Madeleine, J., Maignan, F., Marchand, M., Marti, O., Mellul, L., Meurdesoif, Y., Mignot, J., Musat, I., Ottlé, C., Peylin, P., Planton, Y., Polcher, J., Rio, C., Rochetin, N., Rousset, C., Sepulchre, P., Sima, A., Swingedouw, D., Thiéblemont, R., Traore, A., Vancoppenolle, M., Vial, J., Vialard, J., Viovy, N., and Vuichard, N. (2020). Presentation and evaluation of the IPSL-CM6A-LR climate model, *Journal of Advances in Modeling Earth Systems*, 12.

Byun, S. K., & Chang, S. D. (1984). Two branches of Tsushima Warm Current in the western channel of the Korea Strait. *한국해양학회지*, 19(2), 200-209.

- Cao, J., Wang, B., Yang, Y.-M., Ma, L., Li, J., Sun, B., Bao, Y., He, J., Zhou, X., and Wu, L. (2018). The NUIST Earth System Model (NESM) version 3: description and preliminary evaluation, *Geosci. Model Dev.*, 11, 2975–2993.
- Cummings, J. A. (2005). Operational multivariate ocean data assimilation. *Quarterly Journal of the Royal Meteorological Society: A journal of the atmospheric sciences, applied meteorology and physical oceanography*, 131(613), 3583-3604.
- Cummings, J. A., & Smedstad, O. M. (2014). Ocean data impacts in global HYCOM. *Journal of Atmospheric and Oceanic Technology*, 31(8), 1771-1791.
- DATA ANALYSIS METHODS IN PHYSICAL OCEANOGRAPHY (2014). Richard E. Thomson and William J. Emery, ELSEVIER, p506-510.
- Egawa, T., Nagata, Y., & Sato, S. (1993). Seasonal variation of the current in the Tsushima Strait deduced from ADCP data of ship-of-opportunity. *Journal of Oceanography*, 49(1), 39-50.
- Eyring, V., S. Bony, G.A. Meehl, C.A. Senior, B. Stevens, R.J. Stouffer and K.E. Taylor, 2016. Overview of the Coupled Model Intercomparison Project Phase 6 (CMIP6) experimental design and organization, *Geosci. Model Dev.*, 9: 1937-1958.

- Fukudome, K. I., Yoon, J. H., Ostrovskii, A., Takikawa, T., & Han, I. S. (2010). Seasonal volume transport variation in the Tsushima Warm Current through the Tsushima Straits from 10 years of ADCP observations. *Journal of oceanography*, 66(4), 539-551.
- G.A. Jacobs, H. T. Perkins, W. J. Teague, and P. J. Hogan (2001). Summer transport through the Tsushima-Korea Strait, *JOURNAL OF GEOPHYSICAL RESEARCH*, VOL. 106, NO. C4, 6917-692.
- Gyundo Pak, Yign Noh, Myong-In Lee, Sang-Wook Yeh, Daehyun Kim, Sang-Yeob Kim, Joon-Lee Lee, Ho Jin Lee, Seung-Hwon Hyun, Kwang-Yeon Lee, Jae-Hak Lee, Young-Gyu Park, Hyunkeun Jin, Hyukmin Park, Young Ho Kim (2021). Korea Institute of Ocean Science and Technology Earth System Model and Its Simulation Characteristics, *Ocean Science Journal*, 56: 18-45.
- H. Perkins, W. J. Teague, and G. A. Jacob (2000). Currents In Korea-Tsushima Strait During Summer 1999, *Geophysical Research Letters*, 27(19), 3033-3036.
- Hong, S. Y., Kwon, Y. C., Kim, T. H., Esther Kim, J. E., Choi, S. J., Kwon, I. H., Kim, J. H., Lee, E. H., Park, R. S. & Kim, D. I. (2018). The Korean Integrated Model (KIM) system for global weather forecasting.

Asia-Pacific Journal of Atmospheric Sciences, 54(1), 267-292.

Isobe, A., Tawara, S., Kaneko, A., & Kawano, M. (1994). Seasonal variability in the Tsushima warm current, Tsushima-Korea Strait. *Continental Shelf Research*, 14(1), 23-35.

Jang, E., Kim, Y. J., Im, J., & Park, Y. G. (2021). Improvement of SMAP sea surface salinity in river-dominated oceans using machine learning approaches. *GIScience & Remote Sensing*, 58(1), 138-160.

Jang, E., Kim, Y. J., Im, J., Park, Y. G., & Sung, T. (2022). Global sea surface salinity via the synergistic use of SMAP satellite and HYCOM data based on machine learning. *Remote Sensing of Environment*, 273, 112980.

Joao Marcos Azevedo Correia de Souza, Phellipe Couto, Rafael Soutelino, Moninya Roughan (2020). Evaluation of four global ocean reanalysis products for New Zealand waters—A guide for regional ocean modelling, *New Zealand Journal of Marine and Freshwater Research*, 55, 132-155.

Kang, B., Hirose, N., & Fukudome, K. I. (2014). Transport variability in the Korea/Tsushima Strait: characteristics and relationship to synoptic atmospheric forcing. *Continental Shelf Research*, 81, 55-66.

Katoh, O., Teshima, K., Kubota, K., & Tsukiyama, K. (1996). Downstream transition of the Tsushima Current west of Kyushu in summer. *Journal of Oceanography*, 52(1), 93-108.

Kawatate, K., Miita, T., Ouchi, Y., & Mizuno, S. (1988). A report on failures of current meter moorings set east of Tsushima Island from 1983 to 1987. *Progress in Oceanography*, 21(3-4), 319-327.

Kelley, M., Schmidt, G. A., Nazarenko, L. S., Bauer, S. E., Ruedy, R., Russell, G. L., Ackerman, A. S., Aleinov, I., Bauer, M., Bleck, R., Canuto, V., Cesana, G., Cheng, Y., Clune, T. L., Cook, B. I., Cruz, C. A., Del Genio, A. D., Elsaesser, G. S., Faluvegi, G., Kiang, N. Y., Kim, D., Lacis, A. A., Leboissetier, A., LeGrande, A. N., Lo, K. K., Marshall, J., Matthews, E. E., McDermid, S., Mezuman, K., Miller, R. L., Murray, L. T., Oinas, V., Orbe, C., García-Pando, C. P., Perlwitz, J. P., Puma, M. J., Rind, D., Romanou, A., Shindell, D. T., Sun, S., Tausnev, N., Tsigaridis, K., Tselioudis, G., Weng, E., Wu, J., and Yao, M.-S., (2020). GISS-E2.1: Configurations and climatology, *Journal of Advances in Modeling Earth Systems*, 12.

Kim, Y. H., Kim, Y. B., Kim, K., Chang, K. I., Lyu, S. J., Cho, Y. K., & Teague, W. J. (2006). Seasonal variation of the Korea Strait Bottom Cold Water and its relation to the bottom current. *Geophysical research letters*, 33(24).

- Kim, S. Y., Park, Y. G., Kim, Y. H., Seo, S., Jin, H., Pak, G., & Lee, H. J. (2021). Origin, Variability, and Pathways of East Sea Intermediate Water in a High-Resolution Ocean Reanalysis. *Journal of Geophysical Research: Oceans*, 126(6), e2020JC017158.
- Kuhlbrodt, T., Jones, C. G., Sellar, A., Storkey, D., Blockley, E., Stringer, M., Hill, R., Graham, T., Ridley, J., Blaker, A., Calvert, D., Copsey, D., Ellis, R., Hewitt, H., Hyder, P., Ineson, S., Mulcahy, J., Siahann, A., and Walton, J. (2018). The low-resolution version of HadGEM3 GC3. 1: Development and evaluation for global climate. *Journal of Advances in Modeling Earth Systems*, 10(11), 2865-2888.
- Large, W. G., & Yeager, S. G. (2004). Diurnal to decadal global forcing for ocean and sea-ice models: The data sets and flux climatologies.
- Lee, S. H., & Choi, B. J. (2015). Vertical structure and variation of currents observed in autumn in the Korea Strait. *Ocean Science Journal*, 50(2), 163-182.
- Lehodey, P., Senina, I., Wibawa, T. A., Titaud, O., Calmettes, B., Conchon, A., Tranchat, B. & Gaspar, P. (2018). Operational modelling of bigeye tuna (*Thunnus obesus*) spatial dynamics in the Indonesian region. *Marine pollution bulletin*, 131, 19-32.

- Liu, Z. J., Nakamura, H., Zhu, X. H., Nishina, A., & Dong, M. (2017). Tidal and residual currents across the northern Ryukyu Island chain observed by ferryboat ADCP. *Journal of Geophysical Research: Oceans*, 122(9), 7198-7217.
- Liu, Z. J., Nakamura, H., Zhu, X. H., Nishina, A., Guo, X., & Dong, M. (2019). Tempo-spatial variations of the Kuroshio current in the Tokara Strait based on long-term ferryboat ADCP data. *Journal of Geophysical Research: Oceans*, 124(8), 6030-6049.
- Liu, Z. J., Zhu, X. H., Nakamura, H., Nishina, A., Wang, M., & Zheng, H. (2021). Comprehensive observational features for the Kuroshio transport decreasing trend during a recent global warming hiatus. *Geophysical Research Letters*, 48(18), e2021GL094169.
- Lyu, S. J., Kim, Y. G., Kim, K., Book, J. W., & Choi, B. H. (2002). Tidal variations in the cable voltage across the Korea Strait. *Journal of the Korean Society of Oceanography*, 37(1), 1-9.
- Lyu, S. J., & Kim, K. (2003). Absolute transport from the sea level difference across the Korea Strait. *Geophysical Research Letters*, 30(6).
- Metzger, E. J., Helber, R. W., Hogan, P. J., Posey, P. G., Thoppil, P. G.,

Townsend, T. L., Wallcraft, A. J., Smedstad, O. M., Franklin, D. S., Zamudo-Lopez, L. & Phelps, M. W. (2017). Global ocean forecast system 3.1 validation test. Naval Research Lab Stennis Detachment Stennis Space Center MS Stennis Space Center United States.

Miller, R. L., Schmidt, G. A., Nazarenko, L., Bauer, S. E., Kelley, M., Ruedy, R., Russell, G. L., Ackerman, A., Aleinov, I., Bauer, M., Bleck, R., Canuto, V., Cesana, G., Cheng, Y., Clune, T. L., Cook, B., Cruz, C. A., Del Genio, A. D., Elsaesser, G. S., Faluvegi, G., Kiang, N. Y., Kim, D., Lacis, A. A., Leboissetier, A., LeGrande, A. N., Lo, K. K., Marshall, J., Matthews, E. E., McDermid, S., Mezuman, K., Murray, L. T., Oinas, V., Orbe, C., García-Pando, C. P., Perlwitz, J. P., Puma, M. J., Rind, D., Romanou, A., Shindell, D. T., Sun, S., Tausnev, N., Tsigaridis, K., Tselioudis, G., Weng, E., Wu, J., and Yao, M.-S. (2021). CMIP6 historical simulations (1850–2014) with GISS ModelE2.1, *Journal of Advances in Modeling Earth Systems*, 13.

Mizuno, S., Kawatate, K., Nagahama, T., & Miita, T. (1989). Measurements of East Tushima Current in winter and estimation of its seasonal variability. *Journal of the Oceanographical Society of Japan*, 45(6), 375-384.

Nitani, H. (1972). Beginning of the Kuroshio. *Kuroshio, Physical Aspect of the Japan Current.*

Ostrovskii A, Fukudome K, Yoon JH, Takikawa T (2009). Variability of the volume transport through the Korea/Tsushima Strait as inferred from the shipborne acoustic Doppler current profiler observations in 1997-2007, *Oceanology* 49(3), 338-349

O'Neill, B.C., C. Tebaldi, D.P. van Vuuren, V. Eyring, P. Friedlingstein, G. Hurtt, R. Knutti, E. Kriegler, J.-F. Lamarque, J. Lowe, G.A. Meehl, R. Moss, K. Riahi and B.M. Sanderson (2016). The Scenario Model Intercomparison Project (ScenarioMIP) for CMIP6. *Geosci. Model Dev.*, 9: 3461-3482.

Riahi, K., van Vuuren, D. P., Kriegler, E., Edmonds, J., O'Neill, B. C., Fujimori, S., Bauer, N., Calvin, K., Dellink, R., Fricko, O., Lutz, W., Popp, A., Cuaresma, J. C. K. C. S., Leimbach, M., Jiang, L., Kram, T., Rao, S., Emmerling, J., Ebi, K., Hasegawa, T., Havlik, P., Humpenöder, F., Da Silva, L. A., Smith, S., Stehfest, E., Bosetti, V., Eom, J., Gernaat, D., Masui, T., Rogelj, J., Strefler, J., Drouet, L., Krey, V., Luderer, G., Harmsen, M., Takahashi, K., Baumstark, L., Doelman, J. C., Kainuma, M., Klimont, Z., Marangoni, G., Lotze-Campen, H., Obersteiner, M., Tabeau, A. & Tavoni, M. (2017). The shared socioeconomic pathways and their energy, land use, and greenhouse gas emissions implications: an overview. *Global environmental change*, 42, 153-168.

Shin, H. R., Lee, J. H., Kim, C. H., Yoon, J. H., Hirose, N., Takikawa, T.,

& Cho, K. (2022). Long-term variation in volume transport of the Tsushima warm current estimated from ADCP current measurement and sea level differences in the Korea/Tsushima Strait. *Journal of Marine Systems*, 232, 103750.

Shinichiro Kida, Katsumi Takayama, Yoshi N. Sasaki, Hiromi Matsuura and Naoki Hirose (2020). Increasing trend in Japan Sea Throughflow transport, *Journal of Oceanography*, 77, 145-53.

Séférian, R., Nabat, P., Michou, M., Saint-Martin, D., Voldoire, A., Colin, J., Decharme, B., Delire, C., Berthet, S., Chevallier, M., Sénési, S., Franchisteguy, L., Vial, J., Mallet, M., Joetzjer, E., Geoffroy, O., Guérémy, J.-F., Moine, M.-P., Msadek, R., Ribes, A., Rocher, M., Roehrig, R., Salas-y-Méllia, D., Sanchez, E., Terray, L., Valcke, S., Waldman, R., Aumont, O., Bopp, L., Deshayes, J., Éthé, C., and Madec, G. (2020). Evaluation of CNRM Earth System Model, CNRM-ESM2-1: Role of Earth System Processes in Present-Day and Future Climate, *Journal of Advances in Modeling Earth Systems*, 11, 4182–4227.

Shinoda, T., Zamudio, L., Guo, Y., Metzger, E. J., & Fairall, C. W. (2019). Ocean variability and air-sea fluxes produced by atmospheric rivers. *Sci Rep* 9: 2152.

Szekely, T., Gourrion, J., Pouliquen, S., & Reverdin, G. (2019). The CORA

5.2 dataset for global in situ temperature and salinity measurements: data description and validation. *Ocean Science*, 15(6), 1601-1614.

Takikawa, T., Yoon, J. H., & Cho, K. D. (2003). Tidal currents in the Tsushima Straits estimated from ADCP data by ferryboat. *Journal of oceanography*, 59(1), 37-47.

Takikawa, T., Yoon, J. H., & Cho, K. D. (2005). The Tsushima Warm Current through Tsushima Straits Estimated from Ferryboat ADCP Data, *Journal of Physical Oceanography*, 35, 1154-1168.

Takikawa, T., & Yoon, J. H. (2005). Volume transport through the Tsushima Straits estimated from sea level difference. *Journal of Oceanography*, 61(4), 699-708.

Teague, W. J., Jacobs, G. A., Perkins, H. T., Book, J. W., Chang, K. I., & Suk, M. S. (2002). Low-frequency current observations in the Korea/Tsushima Strait. *Journal of Physical Oceanography*, 32(6), 1621-1641.

Teague, W. J., Ko, D. S., Jacobs, G. A., Perkins, H. T., Book, J. W., Smith, S. R., Chang K. I., Suk M. S., Kim K. , Lyu S. J. and Tang, T. Y (2006). Currents Through the Korea/Tsushima Strait, *Oceanography*, 19(3), 51-63.

Tebaldi, C., K. Debeire, V. Eyring, E. Fischer, J. Fyfe, P. Friedlingstein, R. Knutti, J. Lowe, B. O'Neill, B. Sanderson, D. van Vuuren, K. Riahi, M. Meinshausen, Z. Nicholls, K.B. Tokarska, G. Hurtt, E. Kriegler, J.-F. Lamarque, G. Meehl, R. Moss, S.E. Bauer, O. Boucher, V. Brovkin, Y.-H. Byun, M. Dix, S. Gualdi, H. Guo, J.G. John, S. Kharin, Y. Kim, T. Koshiro, L. Ma, D. Olivié, S. Panickal, F. Qiao, X. Rong, N. Rosenbloom, M. Schupfner, R. Séférian, A. Sellar, T. Semmler, X. Shi, Z. Song, C. Steger, R. Stouffer, N. Swart, K. Tachiiri, Q. Tang, H. Tatebe, A. Voldoire, E. Volodin, K. Wyser, X. Xin, S. Yang, Y. Yu and Ziehn, T., (2021). Climate model projections from the scenario model intercomparison project (ScenarioMIP) of CMIP6. *Earth System Dynamics*, 12(1), 253-293.

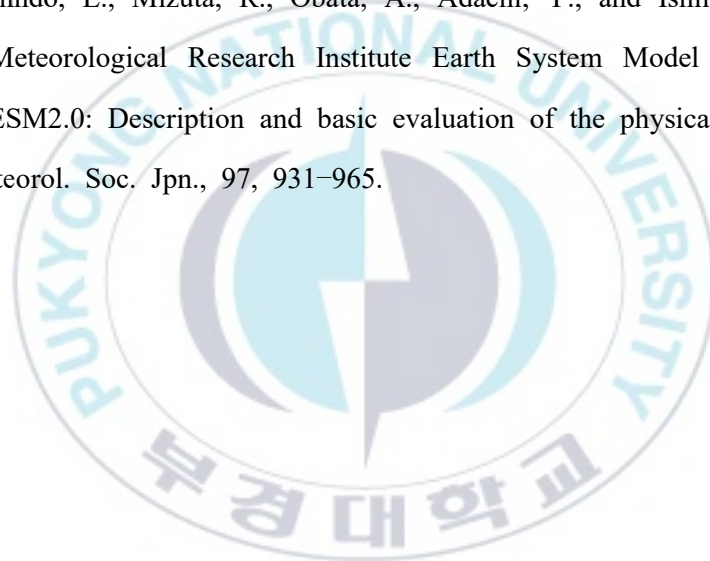
Wu, T., Lu, Y., Fang, Y., Xin, X., Li, L., Li, W., Jie, W., Zhang, J., Liu, Y., Zhang, L., Zhang, F., Zhang, Y., Wu, F., Li, J., Chu, M., Wang, Z., Shi, X., Liu, X., Wei, M., Huang, A., Zhang, Y., and Liu, X. (2019). The Beijing Climate Center Climate System Model (BCC-CSM): the main progress from CMIP5 to CMIP6, *Geosci. Model Dev.*, 12, 1573–1600.

Xin, X.-G., Wu, T.-W., Zhang, J., Zhang, F., Li, W.-P., Zhang, Y.-W., Lu, Y.-X., Fang, Y.-J., Jie, W.-H., Zhang, L., Dong, M., Shi, X.-L., Li, J.-L., Chu, M., Liu, Q.-X., and Yan, J.-H. (2019). Introduction of BCC models and its participation in CMIP6. *Advances in Climate Change Research*,

15(5), 533.

Yi, S. U. (1966). Seasonal and secular variations of the water volume transport across the Korea Strait. 한국해양학회지, 1(1\_2), 7-13.

Yukimoto, S., Kawai, H., Koshiro, T., Oshima, N., Yoshida, K., Urakawa, S., Tsujino, H., Deushi, M., Tanaka, T., Hosaka, M., Yabu, S., Yoshimura, H., Shindo, E., Mizuta, R., Obata, A., Adachi, Y., and Ishii, M. (2019). The Meteorological Research Institute Earth System Model version 2.0, MRI-ESM2.0: Description and basic evaluation of the physical component, J. Meteorol. Soc. Jpn., 97, 931–965.



## Acknowledgements

이 논문의 완성되기까지 많은 분들의 지도와 격려가 있었음을 기억하기 위해 감사의 마음을 글로 남고자합니다. 먼저, 부족한 실력임에도 불구하고 옆에서 끊임 없이 가르침을 주셨던 김영호 교수님께 감사의 마음을 전하고자 합니다. 2년동안 연구과정 중 수많은 실수가 있었음에도 지도를 아끼지 않으셨던 교수님께서 계셔서 연구원으로서 더 성장할 수 있었습니다. 교수님께 지도를 받을 수 있어서 영광이었습니다. 그리고 바쁘신 와중에 시간을 내어 많은 피드백을 주신 김영규 박사님께도 감사의 말씀을 올립니다. 박사님께서 주셨던 피드백으로 부족했던 부분을 인지하고 한걸음 더 나아갈 수 있었습니다. 또, 제 학위 논문의 심사위원장을 맡아 세세한 피드백을 해주셨던 박재형 교수님께도 감사의 말씀을 올리고 싶습니다. 주셨던 피드백을 수용하는 과정에서 성장하고 있다는 것을 느낄 수 있었습니다. 해양학과 교수님들 및 연구를 위해 도움을 주셨던 모든 분들께도 감사드립니다. 저와 모든 생활을 같이 했던 OPPL 덕분에 행복한 추억을 쌓을 수 있었습니다. 승현이 오빠, 인성이, 나영이, 수민, 수지, 혜민, 난다, 호찬, 금주와 함께 해서 어려움도 극복할 수 있었습니다. 그동안 부족했던 저와 함께 해주어서 감사합니다. 무조건적인 사랑을 주셨던 아버지 정민현, 어머니 류미연 덕분에 지금의 제가 있을 수 있었습니다. 몸만 큰 어린 아이의 어리광을 받아주셔서 늘 감사합니다. 멀리서 응원해주었던 동생 유정도 고맙습니다. 그리고 옆에서 묵묵히 날 챙겨줬던 나의 친구들 소은, 재림 고마워.

2년 동안 많은 것들을 배울 수 있음에도 불구하고, 더 열심히 하지 못해 후회했던 순간이 있어 아쉬움이 있습니다. 낮은 궁금함은 깊은 밤이 되어서야 답이 되어 찾아오는 순간이 많았지만 그 과정이 좋았습니다. 앞으로는 좀 더 이성적으로 행동해야하는 순간이 많겠지만, 그래도 늘 따뜻함을 가진 사람이 되겠습니다.